A FAMILY OF THREE-DIMENSIONAL VIRTUAL ELEMENTS WITH APPLICATIONS TO MAGNETOSTATICS

L. BEIRÃO DA VEIGA*, F. BREZZI†, F. DASSI‡, L. D. MARINI§, AND A. RUSSO¶

Abstract. We consider, as a simple model problem, the application of Virtual Element Methods (VEM) to the linear Magnetostatic three-dimensional problem in the formulation of F. Kikuchi. In doing so, we also introduce new serendipity VEM spaces, where the serendipity reduction is made only on the faces of a general polyhedral decomposition (assuming that internal degrees of freedom could be more easily eliminated by static condensation). These new spaces are meant, more generally, for the combined approximation of H^1-conforming (0-forms), $H(\mathbf{curl})$-conforming (1-forms), and $H(\mathrm{div})$-conforming (2-forms) functional spaces in three dimensions, and they could surely be useful for other problems and in more general contexts.

Key words. Virtual Element Methods, Serendipity, Magnetostatic problems,

AMS subject classifications. 65N30

1. Introduction.

The aim of this paper is two-fold. We present a variant of the serendipity nodal, edge, and face Virtual Elements presented in [12] that could be used in many different applications (in particular since they can be set in an exact sequence), and we show their use on a model linear Magnetostatic problem in three dimensions, following the formulation of F. Kikuchi [36], [35]. Even though such formulation is not widely used within the Electromagnetic computational community, we believe that is it a very nice example of use of the De Rham diagram (see e.g. [27]) that here is available for serendipity spaces of general order.

Virtual Elements were introduced a few years ago [5, 8, 9], and can be seen as part of the wider family of Galerkin approximations based on polytopal decompositions, including Mimetic Finite Difference methods (the *ancestors* of VEM: see e.g. [37, 13] and the references therein), Discontinuous Galerkin (see e.g. [2, 24], or recently [29], and the references therein), Hybridizable Discontinuous Galerkin and their variants (see [26], or much more recently [25, 28], and the references therein). On the other hand their use of non-polynomial basis functions connect them as well with other methods such as polygonal interpolant basis functions, barycentric coordinates, mean value coordinates, metric coordinate method, natural neighbor-based coordinates, generalized FEMs, and maximum entropy shape functions. See for instance [45], [33], [43], [44] and the references therein. Finally, many aspects are closely connected with Finite Volumes and related methods (see e.g. [31], [30], and the references therein).

The list of VEM contributions in the literature is nowadays quite large; in addition to the ones above, we here limit ourselves to mentioning [15, 3, 7, 17, 21, 34, 22, 39, 46, 47].

Here we deal, as a simple model problem, with the classical magnetostatic problem in a smooth-enough bounded domain Ω in $\mathbb{R}^3$, simply connected, with connected

*Department of Mathematics and Applications, University of Milano–Bicocca, Via Cozzi 55, I-20153, Milano, Italy and IMATI-CNR, Via Ferrata 5 27100 Pavia, Italy (lourenco.beirao@unimib.it).

†IMATI-CNR, Via Ferrata 5 27100 Pavia, Italy, (brezzi@imati.cnr.it).

‡Department of Mathematics and Applications, University of Milano–Bicocca, Via Cozzi 55, I-20153, Milano, Italy (franco.dassi@unimib.it).

§Dipartimento di Matematica, University of Pavia and IMATI-CNR, Via Ferrata 1, 27100 Pavia, Italy (marini@imati.cnr.it).

¶Department of Mathematics and Applications, University of Milano–Bicocca, Via Cozzi 55, I-20153, Milano, Italy and IMATI-CNR, Via Ferrata 5 27100 Pavia, Italy (alessandro.russo@unimib.it).

boundary: given $\boldsymbol{j} \in H_0(\mathrm{div};\Omega)$ with $\mathrm{div}\boldsymbol{j} = 0$ in Ω, and given $\mu = \mu(\boldsymbol{x})$ with $0 < \mu_0 \le \mu \le \mu_1$,

$$\begin{cases} \text{find } \boldsymbol{H} \in H(\mathbf{curl};\Omega) \text{ and } \boldsymbol{B} \in H(\mathrm{div};\Omega) \text{ such that:} \\ \mathbf{curl}\boldsymbol{H} = \boldsymbol{j} \text{ and } \mathrm{div}\boldsymbol{B} = 0, \text{ with } \boldsymbol{B} = \mu\boldsymbol{H} \text{ in } \Omega, \\ \text{with the boundary conditions } \boldsymbol{H} \wedge \boldsymbol{n} = 0 \text{ on } \partial\Omega. \end{cases} \tag{1.1}$$

When discretizing a three-dimensional problem, the degrees of freedom internal to elements (tetrahedra, hexahedra, polyhedra, etc.) can, in most cases, be easily eliminated by *static condensation*, and their burden on the resolution of the final linear system is not overwhelming. This is not the case for edges and faces, where static condensation would definitely be much more problematic. On edges one cannot save too much: in general the trial and test functions, there, are just one-dimensional polynomials. On faces, however, for 0-forms and 1-forms, higher order approximations on polygons with many edges find a substantial benefit by the use of the serendipity approach, that allows an important saving of degrees of freedom internal to faces.

For that we constructed serendipity virtual elements in [10] and [12] (for scalar or vector valued local spaces, respectively) that however were not fully adapted to the construction of De Rham complexes. The spaces were therefore modified, for the 2d case, in [4]. Here we use this latest version on the *boundary* of the polyhedra of our three-dimensional decompositions, and we show that this can be a quite viable choice.

We point out that, contrary to what happens for FEMs (where, typically, the serendipity subspaces do not depend on the degrees of freedom used in the bigger, non-serendipity, spaces), for Virtual Elements the construction of the serendipity spaces depends, in general, heavily on the degrees of freedom used, so that if we want an exact sequence the *degrees of freedom* in the VEM spaces must be chosen properly.

We will show that the present serendipity VEM spaces are perfectly suited for the approximation of problem (1.1) with the Kikuchi approach, and we believe that they might be quite interesting in many other problems in Electromagnetism as well as in other important applications of Scientific Computing. In particular we have *a whole family* of spaces of different order of accuracy k. For simplicity we assumed here that the same order k is used in all the elements of the decomposition, but we point out that the great versatility of VEM would very easily comply with the use of different orders in different elements, allowing very effective *h-p* strategies.

A single (lowest order only, and particularly cheap) Virtual Element Method for electro-magnetic problems was already proposed in [6], but the family proposed here does not include it: roughly speaking, the element in [6] is based on a generalization to polyhedra of the *lowest order Nédélec first type* element (say, of degree between 0 and 1), while, instead, the family presented here could be seen as being based on generalizations to polyhedra of the *Nédélec second type* elements (of order $k \ge 1$).

A layout of the paper is as follows: in Section 2 we introduce some basic notation, and recall some well known properties of polynomial spaces. In Section 3 we will first recall the Kikuchi variational formulation of (1.1). Then, in Subsection 3.2 we present the *local* two-dimensional Virtual Element spaces of *nodal* and *edge* type to be used on the interelement boundaries. As we mentioned already, *the spaces* are the same already discussed in [5], [1] and in [20], [9], respectively, but with a different choice of the *degrees of freedom*, suitable for the serendipity construction discussed in Subsection 3.3. In Subsection 3.4 we present the *local* three-dimensional spaces. In Subsection 3.5 we construct the *global* version of all these spaces, and discuss their properties and the properties of the relative exact sequence. In Section 4 we first introduce the discretized problem, and in Subsection 4.3 we prove the a priori error bounds for it. In Section 5 we present some numerical results that show that the quality of the approximation is very good, and also that the serendipity variant does not jeopardize the accuracy.

2. Notation and well known properties of polynomial spaces.

In two dimensions, we will denote by $\boldsymbol{x}$ the indipendent variable, using $\boldsymbol{x} = (x, y)$ or (more often) $\boldsymbol{x} = (x_1, x_2)$ following the circumstances. We will also use $\boldsymbol{x}^\perp := (-x_2, x_1)$, and in general, for a vector $\boldsymbol{v} \equiv (v_1, v_2)$,

$$\boldsymbol{v}^\perp := (-v_2, v_1). \tag{2.1}$$

Moreover, for a vector $\boldsymbol{v}$ and a scalar q we will write

$$\mathrm{rot}\boldsymbol{v} := \frac{\partial v_2}{\partial x} - \frac{\partial v_1}{\partial y}, \qquad \mathbf{rot}\, q := \Big(\frac{\partial q}{\partial y}, -\frac{\partial q}{\partial x}\Big). \tag{2.2}$$

We recall some commonly used functional spaces. On a domain $\mathcal{O}$ we have

$$\begin{aligned}
&H(\mathrm{div};\mathcal{O}) = \{\boldsymbol{v} \in [L^2(\mathcal{O})]^3 \text{ with } \mathrm{div}\boldsymbol{v} \in L^2(\mathcal{O})\},\\
&H_0(\mathrm{div};\mathcal{O}) = \{\boldsymbol{\varphi} \in H(\mathrm{div};\mathcal{O}) \text{ s.t. } \boldsymbol{\varphi}\cdot\boldsymbol{n} = 0 \text{ on } \partial\mathcal{O}\},\\
&H(\mathbf{curl};\mathcal{O}) = \{\boldsymbol{v} \in [L^2(\mathcal{O})]^3 \text{ with } \mathbf{curl}\boldsymbol{v} \in [L^2(\mathcal{O})]^3\},\\
&H_0(\mathbf{curl};\mathcal{O}) = \{\boldsymbol{v} \in H(\mathbf{curl};\mathcal{O}) \text{ with } \boldsymbol{v}\wedge\boldsymbol{n} = 0 \text{ on } \partial\mathcal{O}\},\\
&H^1(\mathcal{O}) = \{q \in L^2(\mathcal{O}) \text{ with } \mathbf{grad}\, q \in [L^2(\mathcal{O})]^3\},\\
&H^1_0(\mathcal{O}) = \{q \in H^1(\mathcal{O}) \text{ with } q = 0 \text{ on } \partial\mathcal{O}\}.
\end{aligned}$$

For an integer $s \geq -1$ we will denote by $\mathbb{P}_s$ the space of polynomials of degree $\leq s$. Following a common convention, $\mathbb{P}_{-1} \equiv \{0\}$ and $\mathbb{P}_0 \equiv \mathbb{R}$. Moreover, for $s \geq 1$

$$\mathbb{P}^h_s := \{\text{homogeneous pol.s in } \mathbb{P}_s\}, \quad \mathbb{P}^0_s(\mathcal{O}) := \{q \in \mathbb{P}_s \text{ s. t. } \int_{\mathcal{O}} q \,\mathrm{d}\mathcal{O} = 0\}. \tag{2.3}$$

The following decompositions of polynomial vector spaces are well known and will be useful in what follows. In two dimensions we have

$$(\mathbb{P}_s)^2 = \mathbf{rot}(\mathbb{P}_{s+1}) \oplus \boldsymbol{x}\mathbb{P}_{s-1} \quad \text{and} \quad (\mathbb{P}_s)^2 = \mathbf{grad}(\mathbb{P}_{s+1}) \oplus \boldsymbol{x}^\perp\mathbb{P}_{s-1}, \tag{2.4}$$

and in three dimension

$$(\mathbb{P}_s)^3 = \mathbf{curl}((\mathbb{P}_{s+1})^3) \oplus \boldsymbol{x}\mathbb{P}_{s-1}, \quad \text{and} \quad (\mathbb{P}_s)^3 = \mathbf{grad}(\mathbb{P}_{s+1}) \oplus \boldsymbol{x}\wedge(\mathbb{P}_{s-1})^3. \tag{2.5}$$

Taking the **curl** of the second of (2.5) we also get :

$$\mathbf{curl}(\mathbb{P}_s)^3 = \mathbf{curl}(\boldsymbol{x}\wedge(\mathbb{P}_{s-1})^3) \tag{2.6}$$

which used in the first of (2.5) gives:

$$(\mathbb{P}_s)^3 = \mathbf{curl}(\boldsymbol{x}\wedge(\mathbb{P}_s)^3) \oplus \boldsymbol{x}\mathbb{P}_{s-1}. \tag{2.7}$$

We also recall the definition of the Nédélec *local* spaces of 1-st and 2-nd kind.

$$\begin{aligned}
&\text{In 2d:} \quad N1_s = \mathbf{grad}\,\mathbb{P}_{s+1} \oplus \boldsymbol{x}^\perp(\mathbb{P}_s)^2,\ s \geq 0, \qquad N2_s := (\mathbb{P}_s)^2,\ s \geq 1,\\
&\text{in 3d:} \quad N1_s = \mathbf{grad}\,\mathbb{P}_{s+1} \oplus \boldsymbol{x}\wedge(\mathbb{P}_s)^3,\ s \geq 0, \qquad N2_s := (\mathbb{P}_s)^3,\ s \geq 1.
\end{aligned} \tag{2.8}$$

In what follows, when dealing with the *faces* of a polyhedron (or of a polyhedral decomposition) we shall use two-dimensional differential operators that act on the restrictions to faces of scalar functions that are defined on a three-dimensional domain. Similarly, for vector valued functions we will use two-dimensional differential operators that act on the restrictions to faces of the tangential components. In many cases, no confusion will be likely to occur; however, to stay on the safe side, we will often use a superscript τ to denote the tangential components of a three-dimensional vector, and a subscript f to indicate the two-dimensional differential operator. Hence, to fix ideas, if a face has equation $x_3 = 0$ then $\boldsymbol{x}^\tau := (x_1, x_2)$ and, say, $\mathrm{div}_f \boldsymbol{v}^\tau := \frac{\partial v_1}{\partial x_1} + \frac{\partial v_2}{\partial x_2}$.

3. The problem and the spaces.

3.1. The Kikuchi variational formulation. Here we shall deal with the variational formulation introduced in [35]. Given $\boldsymbol{j} \in H_0(\mathrm{div};\Omega)$ with $\mathrm{div}\boldsymbol{j} = 0$,

$$\begin{cases} \text{find } \boldsymbol{H} \in H_0(\mathbf{curl};\Omega) \text{ and } p \in H^1_0(\Omega) \text{ such that:} \\ \int_\Omega \mathbf{curl}\boldsymbol{H}\cdot\mathbf{curl}\boldsymbol{v}\,\mathrm{d}\Omega + \int_\Omega \nabla p\cdot\mu\boldsymbol{v}\,\mathrm{d}\Omega = \int_\Omega \boldsymbol{j}\cdot\mathbf{curl}\boldsymbol{v}\,\mathrm{d}\Omega \quad \forall \boldsymbol{v} \in H_0(\mathbf{curl};\Omega) \\ \int_\Omega \nabla q\cdot\mu\boldsymbol{H}\,\mathrm{d}\Omega = 0 \quad \forall q \in H^1_0(\Omega). \end{cases} \tag{3.1}$$

It is easy to check that (3.1) has a unique solution $(\boldsymbol{H}, p)$. Then we check that $\boldsymbol{H}$ and $\mu\boldsymbol{H}$ give the solution of (1.1) and $p = 0$. Checking that $p = 0$ is immediate, just taking $\boldsymbol{v} = \nabla p$ in the first equation. Once we know that $p = 0$ the first equation gives $\mathbf{curl}\boldsymbol{H} = \boldsymbol{j}$, and then the second equation gives $\mathrm{div}\mu\boldsymbol{H} = 0$.

We will now design the Virtual Element approximation of (3.1) of order $k \geq 1$. We define first the local spaces. Let P be a polyhedron, simply connected, with all its faces also simply connected and convex. (For the treatment of non-convex faces we refer to [12]). More detailed assumptions will be given in Section 4.3.

3.2. The local spaces on faces. We first recall the local *nodal* and *edge* spaces on faces introduced in [4]. We shall deal with a sort of generalisation to polygons of *Nédélec elements of the second kind* $N2$ (see (2.8)). For this, let $k \geq 1$. For each face f of P, the *edge* space on f is defined as

$$V^{\mathrm{e}}_k(f) := \Big\{\boldsymbol{v} \in [L^2(f)]^2 : \mathrm{div}\boldsymbol{v} \in \mathbb{P}_k(f),\ \mathrm{rot}\boldsymbol{v} \in \mathbb{P}_{k-1}(f),\ \boldsymbol{v}\cdot\boldsymbol{t}_e \in \mathbb{P}_k(e)\,\forall e \subset \partial f\Big\}, \tag{3.2}$$

with the degrees of freedom

$$\bullet \text{ on each } e \subset \partial f, \text{ the moments } \int_e (\boldsymbol{v}\cdot\boldsymbol{t}_e) p_k\,\mathrm{d}s \quad \forall p_k \in \mathbb{P}_k(e), \tag{3.3}$$

$$\bullet \text{ the moments } \int_f \boldsymbol{v}\cdot\boldsymbol{x}_f\, p_k\,\mathrm{d}f \quad \forall p_k \in \mathbb{P}_k(f), \tag{3.4}$$

$$\bullet \int_f \mathrm{rot}\boldsymbol{v}\ p^0_{k-1}\,\mathrm{d}f \quad \forall p^0_{k-1} \in \mathbb{P}^0_{k-1}(f) \qquad (\text{only for } k > 1)), \tag{3.5}$$

where $\boldsymbol{x}_f = \boldsymbol{x} - \mathbf{b}_f$, with $\mathbf{b}_f$ = barycenter of f, and $\mathbb{P}^0_s$ was defined in (2.3).

We recall that for $\boldsymbol{v} \in V^{\mathrm{e}}_k(f)$ the value of $\mathrm{rot}\boldsymbol{v}$ is easily computable from the degrees of freedom (3.3) and (3.5). Indeed, the mean value of $\mathrm{rot}\boldsymbol{v}$ on f is computable from (3.3) and Stokes Theorem, and then (since $\mathrm{rot}\boldsymbol{v} \in \mathbb{P}_{k-1}$) the use of (3.5) gives the full value of $\mathrm{rot}\boldsymbol{v}$. Once we know $\mathrm{rot}\boldsymbol{v}$, following [4], we can easily compute, always for each $\boldsymbol{v} \in V^{\mathrm{e}}_k(f)$, the L^2–projection $\Pi^0_{k+1} : V^{\mathrm{e}}_k(f) \to [\mathbb{P}_{k+1}(f)]^2$. Indeed: by definition of projection, using (2.4) and integrating by parts we obtain:

$$\begin{aligned} \int_f \Pi^0_{k+1}\boldsymbol{v}\cdot\mathbf{p}_{k+1}\,\mathrm{d}f &:= \int_f \boldsymbol{v}\cdot\mathbf{p}_{k+1}\,\mathrm{d}f = \int_f \boldsymbol{v}\cdot(\mathbf{rot}\,q_{k+2} + \boldsymbol{x}_f q_k)\,\mathrm{d}f \\ &= \int_f (\mathrm{rot}\boldsymbol{v}) q_{k+2}\,\mathrm{d}f + \sum_{e\subset\partial f}\int_e (\boldsymbol{v}\cdot\boldsymbol{t}) q_{k+2}\,\mathrm{d}s + \int_f \boldsymbol{v}\cdot\boldsymbol{x}_f q_k\,\mathrm{d}f \end{aligned} \tag{3.6}$$

and it is immediate to check that each of the last three terms is computable.

Remark 3.1. Among other things, projection operators can be used to define suitable scalar products in $V_k^{\rm e}(f)$. As common in the virtual element literature, we could use the (Hilbert) norm

$$\|\boldsymbol{v}\|^2_{V_k^{\rm e}(f)} := \|\Pi^0_k \boldsymbol{v}\|^2_{0,f} + \sum_i (dof_i\{(I-\Pi^0_k)\boldsymbol{v}\})^2, \tag{3.7}$$

where the dof_i are the degrees of freedom in $V_k^{\rm e}(f)$, properly scaled. In (3.7) we could also insert any symmetric and positive definite matrix S and change the second term into $\mathbf{d}^T\, S\, \mathbf{d}$ (with $\mathbf{d}=$ the vector of the $dof_i\{(I-\Pi^0_k)\boldsymbol{v}\}$). Alternatively we could use

$$\|\boldsymbol{v}\|^2_{V_k^{\rm e}(f)} := \|\Pi^0_{k+1}\boldsymbol{v}\|^2_{0,f} + h_f\|(I-\Pi^0_{k+1})\boldsymbol{v}\cdot\boldsymbol{t}\|^2_{0,\partial f} \tag{3.8}$$

(that is clearly a Hilbert norm) where h_f is the diameter of the face f. It is easy to check that the associated inner product *scales* like the natural $[L^2(f)]^2$ inner product (meaning that $\|\boldsymbol{v}\|_{V_k^{\rm e}(f)}$ is bounded above and below by $\|\boldsymbol{v}\|_{0,f}$ times suitable constants independent of h_f), and moreover coincides with the $[L^2(f)]^2$ inner product whenever one of the two entries is in $(\mathbb{P}_{k+1})^2$.

For each face f of P, the *nodal* space of order $k+1$ is defined as

$$V^{\rm n}_{k+1}(f) := \Big\{q \in H^1(f):\ q_{|e} \in \mathbb{P}_{k+1}(e)\ \forall e \subset \partial f,\ \Delta q \in \mathbb{P}_k(f)\Big\}, \tag{3.9}$$

with the degrees of freedom

- (3.10) for each vertex ν the value $q(\nu)$,
- (3.11) for each edge e the moments $\int_e q\, p_{k-1}\,{\rm d}s \quad \forall p_{k-1} \in \mathbb{P}_{k-1}(e)$,
- (3.12) $\int_f (\nabla q \cdot \boldsymbol{x}_f)\, p_k\,{\rm d}f \quad \forall p_k \in \mathbb{P}_k(f)$.

3.3. The local serendipity spaces on faces.

We recall the serendipity spaces introduced in [4], which will be used to construct the serendipity spaces on polyhedra. Let f be a face of P, assumed to be a convex polygon. Following [10] we introduce

$$\beta := k+1-\eta. \tag{3.13}$$

where η is *the number of straight lines necessary to cover the boundary of* f. We note that the convexity of f does not imply that η is equal to the number of edges of f, since we might have different consecutive edges that belong to the same straight line. Next, we define a projection $\Pi^{\rm e}_S : V_k^{\rm e}(f) \to [\mathbb{P}_k(f)]^2$ as follows:

$$\int_{\partial f} [(\boldsymbol{v}-\Pi^{\rm e}_S\boldsymbol{v})\cdot\boldsymbol{t}][\nabla p\cdot\boldsymbol{t}]\,{\rm d}s = 0 \quad \forall p \in \mathbb{P}_{k+1}(f), \tag{3.14}$$

$$\int_{\partial f} (\boldsymbol{v}-\Pi^{\rm e}_S\boldsymbol{v})\cdot\boldsymbol{t}\,{\rm d}s = 0, \tag{3.15}$$

$$\int_f {\rm rot}(\boldsymbol{v}-\Pi^{\rm e}_S\boldsymbol{v})p^0_{k-1}\,{\rm d}f = 0 \quad \forall p^0_{k-1} \in \mathbb{P}^0_{k-1}(f) \quad \text{for } k>1, \tag{3.16}$$

$$\int_f (\boldsymbol{v}-\Pi^{\rm e}_S\boldsymbol{v})\cdot\boldsymbol{x}_f\, p_\beta\,{\rm d}f \quad \forall p_\beta \in \mathbb{P}_\beta(f) \quad \textbf{only for } \beta \ge 0. \tag{3.17}$$

The **serendipity edge space** is then defined as:

$$SV_k^{\rm e}(f) := \Big\{\boldsymbol{v} \in V_k^{\rm e}(f)\ :\ \int_f (\boldsymbol{v}-\Pi^{\rm e}_S\boldsymbol{v})\cdot\boldsymbol{x}_f\, p\,{\rm d}f = 0 \quad \forall p \in \mathbb{P}_{\beta|k}(f)\Big\}, \tag{3.18}$$

where $\mathbb{P}_{\beta|k}$ is the space spanned by all the homogeneous polynomials of degree s with $\beta < s \le k$. The degrees of freedom in $SV_k^{\rm e}(f)$ will be (3.3) and (3.5), plus

$$\int_f \boldsymbol{v}\cdot\boldsymbol{x}_f\, p_\beta\,{\rm d}f \quad \forall p_\beta \in \mathbb{P}_\beta(f) \qquad \textbf{only if } \beta \ge 0. \tag{3.19}$$

To summarize: if $\beta < 0$, i.e., if $k+1 < \eta$, the only internal degrees of freedom are (3.5), and the moments (3.4) are given by those of $\Pi^{\rm e}_S$. Instead, for $\beta \geq 0$ we have to include among the d.o.f. the moments of order up to β given in (3.19). The remaining moments, of order up to k, are again given by those of $\Pi^{\rm e}_S$. We point out that, on triangles, these are now exactly the Nédélec elements of second kind.

Clearly in $SV^{\rm e}_k(f)$ (that is included in $V^{\rm e}_k(f)$) we can still use the scalar product defined in (3.8) or (3.7).

For the construction of the *nodal* serendipity space we proceed as before. Let $\Pi^{\rm n}_S : V^{\rm n}_{k+1}(f) \to \mathbb{P}_{k+1}(f)$ be a projection defined by

$$
\begin{cases}
\int_{\partial f} \partial_t (q - \Pi^{\rm n}_S q) \partial_t p \,{\rm d}s = 0 \quad \forall p \in \mathbb{P}_{k+1}(f),\\
\int_{\partial f} (\boldsymbol{x}_f \cdot \boldsymbol{n})(q - \Pi^{\rm n}_S q)\,{\rm d}s = 0,\\
\int_f (\nabla(q - \Pi^{\rm n}_S q) \cdot \boldsymbol{x}_f \, p_\beta \,{\rm d}f = 0 \quad \forall p_\beta \in \mathbb{P}_\beta(f) \quad \textbf{only} \text{ for } \beta \geq 0.
\end{cases} \tag{3.20}
$$

The **serendipity nodal space** is then defined as:

$$
SV^{\rm n}_{k+1}(f) := \Big\{ q \in V^{\rm n}_{k+1}(f) \,:\, \int_f (\nabla q - \nabla \Pi^{\rm n}_S q) \cdot \boldsymbol{x}_f \, p \,{\rm d}f = 0 \,\forall p \in \mathbb{P}_{\beta|k}(f) \Big\}. \tag{3.21}
$$

The degrees of freedom in $SV^{\rm n}_{k+1}(f)$ will be (3.10) and (3.11), plus

$$
\int_f (\nabla q \cdot \boldsymbol{x}_f)\, p_\beta \,{\rm d}f \quad \forall p_\beta \in \mathbb{P}_\beta(f) \qquad \textbf{only if } \beta \geq 0. \tag{3.22}
$$

From this construction it follows that the nodal serendipity space contains internal d.o.f. only if $k+1 \geq \eta$, and the number of these d.o.f. is equal to the dimension of $\mathbb{P}_\beta$ only. The remaining d.o.f. are copied from those of $\Pi^{\rm n}_S$. Note also that on triangles we have back the old polynomial Finite Elements of degree $k+1$. Before dealing with the three dimensional spaces, we recall a useful result proven in [4], Proposition 5.4.

Proposition 3.2. It holds

$$
\nabla SV^{\rm n}_{k+1}(f) = \{\boldsymbol{v} \in SV^{\rm e}_k(f) :\ {\rm rot}\boldsymbol{v} = 0\}. \tag{3.23}
$$

The following result is immediate, but we point it out for future use.

Proposition 3.3. For every $q \in V^{\rm n}_{k+1}(f)$ there exists a (unique) q^* such that

$$
q^* \in SV^{\rm n}_{k+1}(f) \quad \text{(and we denote it as } q^* = \sigma^{{\rm n},f}(q)), \tag{3.24}
$$

that has the same degrees of freedom (3.10),(3.11), and (3.22) of q. The difference $q - q^*$ is obviously a bubble in $V^{\rm n}_{k+1}(f)$. Similarly, for a $\boldsymbol{v}$ in $V^{\rm e}_k(f)$ there exists a unique $\boldsymbol{v}^*$ with

$$
\boldsymbol{v}^* \in SV^{\rm e}_k(f) \quad \text{(and we denote it as } \boldsymbol{v}^* = \sigma^{{\rm e},f}(\boldsymbol{v})), \tag{3.25}
$$

with the same degrees of freedom (3.3)-(3.5), and (3.19) of $\boldsymbol{v}$. The difference $\boldsymbol{v} - \boldsymbol{v}^*$ is an $H(rot)$-bubble and, in particular, is the gradient of a scalar bubble $\xi(\boldsymbol{v})$:

$$
\nabla \xi \equiv \boldsymbol{v} - \boldsymbol{v}^*. \tag{3.26}
$$

Proof. It is clear from the previous discussion that the degrees of freedom (3.10), (3.11), and (3.22) determine q^* in a unique way. As q and q^* share the same boundary degrees of freedom (3.10) and (3.11), they will coincide on the whole boundary ∂f, so that $q - q^*$ is a bubble. Similarly, given $\boldsymbol{v}$ in $V_k^{\rm e}(f)$ the degrees of freedom (3.3)-(3.5), and (3.19) determine uniquely a $\boldsymbol{v}^*$ in $SV_k^{\rm e}(f)$. The two vector valued functions $\boldsymbol{v}$ and $\boldsymbol{v}^*$, sharing the degrees of freedom (3.3)-(3.5) must have the same tangential components on ∂f and *the same* rot. In particular, $\mathrm{rot}(\boldsymbol{v}-\boldsymbol{v}^*) = 0$ and (as f is simply connected) $\boldsymbol{v} - \boldsymbol{v}^*$ must be a gradient of some scalar function ξ (that we can take as a bubble, since its tangential derivative on ∂f is zero). □

3.4. The local spaces on polyhedra. Let P be a polyhedron, simply connected with all its faces simply connected and convex. For each face f we will use the serendipity spaces $SV_{k+1}^{\rm n}(f)$ and $SV_k^{\rm e}(f)$ as defined in (3.21) and (3.18), respectively. We then introduce the three-dimensional analogues of (3.21) and (3.18), that are

$$(3.27)\quad V_k^{\rm e}(\mathrm{P}) := \Big\{\boldsymbol{v} \in [L^2(\mathrm{P})]^3\ : \mathrm{div}\boldsymbol{v} \in \mathbb{P}_{k-1}(\mathrm{P}),\ \mathbf{curl}(\mathbf{curl}\boldsymbol{v}) \in [\mathbb{P}_k(\mathrm{P})]^3,$$
$$\boldsymbol{v}^{\tau}_{|f} \in SV_k^{\rm e}(f)\ \forall \text{ face } f \subset \partial\mathrm{P},\ \boldsymbol{v}\cdot\boldsymbol{t}_e \text{ continuous on each edge } e \subset \partial\mathrm{P}\Big\},$$

$$(3.28)\quad V_{k+1}^{\rm n}(\mathrm{P}) := \Big\{q \in C^0(\mathrm{P})\ : q_{|f} \in SV_{k+1}^{\rm n}(f) \quad \forall \text{ face } f \subset \partial\mathrm{P},\ \Delta\, q \in \mathbb{P}_{k-1}(\mathrm{P})\Big\}.$$

This time however we will also need a Virtual Element *face* space (for the discretization of two-forms), that we define as

$$(3.29)\ V_{k-1}^{\rm f}(\mathrm{P}) := \Big\{\boldsymbol{w} \in [L^2(\mathrm{P})]^3 : \mathrm{div}\boldsymbol{w} \in \mathbb{P}_{k-1},\ \mathbf{curl}\boldsymbol{w} \in [\mathbb{P}_k]^3,\ \boldsymbol{w}\cdot\boldsymbol{n}_f \in \mathbb{P}_{k-1}(f)\ \forall f\Big\}.$$

Remark 3.4. We note that in several cases, in particular for polyhedra with many faces, the number of *internal* degrees of freedom for the spaces (3.27), (3.28), and (3.29) will be *more than necessary*. However, at this point, we will not make efforts to diminish them, as we assume that in practice we could eliminate them by static condensation (or even construct suitable serendipity variants).

Among the same lines of Proposition 3.3, we have now:

Proposition 3.5. For every function q in the (non serendipity!) space

$$(3.30)\quad \widetilde{V}_{k+1}^{\rm n}(\mathrm{P}) := \Big\{q \in C^0(\mathrm{P})\ :\ q_{|f} \in V_{k+1}^{\rm n}(f)\ \forall \text{ face } f \subset \partial\mathrm{P},\ \text{and } \Delta q \in \mathbb{P}_{k-1}\Big\}$$

there exists exactly one element $q^* = \sigma^{\rm n,P}(q)$ in $V_{k+1}^{\rm n}(\mathrm{P})$ such that

$$(3.31)\qquad q^*_{|f} = \sigma^{{\rm n},f}(q_{|f}) \qquad \forall \text{ face } f, \quad \text{and} \qquad \Delta(q-q^*) = 0 \text{ in P}.$$

Similarly, for every vector-valued function $\boldsymbol{v}$ in the (non serendipity!) space

$$(3.32)\quad \widetilde{V}_k^{\rm e}(\mathrm{P}) := \Big\{\boldsymbol{v} \in [L^2(\mathrm{P})]^3\ : \mathrm{div}\boldsymbol{v} \in \mathbb{P}_{k-1}(\mathrm{P}),\ \mathbf{curl}(\mathbf{curl}\boldsymbol{v}) \in [\mathbb{P}_k(\mathrm{P})]^3$$
$$\boldsymbol{v}^{\tau}_{|f} \in V_k^{\rm e}(f)\ \forall \text{ face } f \subset \partial\mathrm{P},\ \boldsymbol{v}\cdot\boldsymbol{t}_e \text{ continuous on each edge } e \subset \partial\mathrm{P}\Big\},$$

there exists exactly one element $\boldsymbol{v}^* = \sigma^{\rm e,P}(\boldsymbol{v})$ of $V_k^{\rm e}(\mathrm{P})$ such that:

$$(3.33)\qquad \bullet \quad \text{on each face } f \text{ of } \partial\mathrm{P} : \quad (\boldsymbol{v}^*)^{\tau} = \sigma^{{\rm e},f}(\boldsymbol{v}^{\tau}) \quad (\text{as defined in (3.25)}),$$

$$(3.34)\qquad \bullet \quad \text{and in P} : \qquad \mathrm{div}(\boldsymbol{v}-\boldsymbol{v}^*) = 0 \quad \text{and} \quad \mathbf{curl}(\boldsymbol{v}-\boldsymbol{v}^*) = \mathbf{0}.$$

Proof. The first part, relative to nodal elements, is obvious: on each face we take as q^* the one given by (3.24) in Proposition 3.3, and then we take $\Delta q^* = \Delta q$ inside. For constructing $\boldsymbol{v}^*$ we also start by defining its tangential components on each face using Proposition 3.3. Now, on each face f we have a (scalar) bubble ξ_f (whose tangential gradient equals the tangential components of $\boldsymbol{v} - \boldsymbol{v}^*$), and we construct in P the scalar function ξ which is: equal to ξ_f on each face f, and harmonic inside P. Then we set $\boldsymbol{v}^* := \boldsymbol{v} + \nabla\xi$, and we check immediately that $\boldsymbol{v}^*$ verifies property (3.33), and also properties (3.34), since ξ vanishes on all edges and is harmonic inside. ∎

Proposition 3.6. It holds

$$\nabla V^{\rm n}_{k+1}(\mathrm{P}) = \{\boldsymbol{v} \in V^{\rm e}_k(\mathrm{P}) : \ \mathbf{curl}\boldsymbol{v} = \mathbf{0}\}. \tag{3.35}$$

Proof. From the above definitions we easily see that the *tangential gradient* of any $q \in V^{\rm n}_{k+1}(\mathrm{P})$, applied *face by face*, belongs to $SV^{\rm e}_k(f)$. Consequently, we also have that $\boldsymbol{v} := \mathbf{grad}q$ belongs to $V^{\rm e}_k(\mathrm{P})$, as $\mathrm{div}\boldsymbol{v} \in \mathbb{P}_{k-1}(\mathrm{P})$ and $\mathbf{curl}\boldsymbol{v} = 0$. Hence,

$$\nabla V^{\rm n}_{k+1}(\mathrm{P}) \subseteq \{\boldsymbol{v} \in V^{\rm e}_k(\mathrm{P}) : \ \mathbf{curl}\boldsymbol{v} = \mathbf{0}\}. \tag{3.36}$$

Conversely, assume that a $\boldsymbol{v} \in V^{\rm e}_k(\mathrm{P})$ has $\mathbf{curl}\boldsymbol{v} = \mathbf{0}$. As P is simply connected we have that $\boldsymbol{v} = \nabla q$ for some $q \in H^1(\mathrm{P})$. On each face f, the tangential gradient of q (equal to $\boldsymbol{v}^\tau$) is in $SV^{\rm e}_k(f)$ (see (3.27)), and since $\mathrm{rot}_f\boldsymbol{v}^\tau = \mathbf{curl}\boldsymbol{v}\cdot\boldsymbol{n}_f \equiv 0$, from (3.23) we deduce that $q_{|f} \in SV^{\rm n}_{k+1}(f)$. Hence, the restriction of q to the boundary of P belongs to $V^{\rm n}_{k+1}(\mathrm{P})_{|\partial\mathrm{P}}$. Moreover, $\Delta q = \mathrm{div}\boldsymbol{v}$ is in $\mathbb{P}_{k-1}(\mathrm{P})$. Hence, $q \in V^{\rm n}_{k+1}(\mathrm{P})$ and the proof is concluded. ∎

In $V^{\rm e}_k(\mathrm{P})$ we have (see [4] and [12]) the degrees of freedom

- (3.37) $\forall$ edge e: $\int_e(\boldsymbol{v}\cdot\boldsymbol{t}_e)p_k\,\mathrm{d}s \quad \forall p_k \in \mathbb{P}_k(e)$,
- (3.38) $\forall$ face f with $\beta_f \geq 0 : \int_f \boldsymbol{v}^\tau\cdot\boldsymbol{x}_f\, p_{\beta_f}\,\mathrm{d}f \quad \forall p_{\beta_f} \in \mathbb{P}_{\beta_f}(f)$,
- (3.39) $\forall$ face f: $\int_f \mathrm{rot}_f\boldsymbol{v}^\tau\, p^0_{k-1}\,\mathrm{d}f \quad \forall p^0_{k-1} \in \mathbb{P}^0_{k-1}(f) \quad$ (for $k > 1$),
- (3.40) $\int_{\mathrm{P}}(\boldsymbol{v}\cdot\boldsymbol{x}_{\mathrm{P}})p_{k-1}\,\mathrm{dP} \quad \forall p_{k-1} \in \mathbb{P}_{k-1}(\mathrm{P})$,
- (3.41) $\int_{\mathrm{P}}(\mathbf{curl}\boldsymbol{v})\cdot(\boldsymbol{x}_{\mathrm{P}}\wedge\mathbf{p}_k)\,\mathrm{dP} \quad \forall \mathbf{p}_k \in [\mathbb{P}_k(\mathrm{P})]^3$,

where β_f = value of β (see (3.13)) on f, and $\boldsymbol{x}_{\mathrm{P}} := \boldsymbol{x} - \mathbf{b}_{\mathrm{P}}$, with $\mathbf{b}_{\mathrm{P}}$ =barycenter of P.

Proposition 3.7. Out of the above degrees of freedom we can compute the $[L^2(\mathrm{P})]^3$ orthogonal projection Π^0_k from $V^{\rm e}_k(\mathrm{P})$ to $[\mathbb{P}_k(\mathrm{P})]^3$.

Proof. Extending the arguments used in [6], and using (2.7) we have that for any $\boldsymbol{p}_k \in (\mathbb{P}_k)^3$ there exist two polynomials, $\boldsymbol{q}_k \in (\mathbb{P}_k)^3$ and $z_{k-1} \in \mathbb{P}_{k-1}$, such that $\boldsymbol{p}_k = \mathbf{curl}(\boldsymbol{x}_{\mathrm{P}}\wedge\mathbf{q}_k) + \boldsymbol{x}_{\mathrm{P}}z_{k-1}$. Hence, from the definition of projection we have:

$$\int_{\mathrm{P}}\Pi^0_k\boldsymbol{v}\cdot\boldsymbol{p}_k\,\mathrm{dP} := \int_{\mathrm{P}}\boldsymbol{v}\cdot\boldsymbol{p}_k\,\mathrm{dP} = \int_{\mathrm{P}}\boldsymbol{v}\cdot\mathbf{curl}(\boldsymbol{x}_{\mathrm{P}}\wedge\boldsymbol{q}_k)\,\mathrm{dP} + \int_{\mathrm{P}}(\boldsymbol{v}\cdot\boldsymbol{x}_{\mathrm{P}})z_{k-1}\,\mathrm{dP}. \tag{3.42}$$

The second integral is given by the d.o.f. (3.40), while for the first one we have, upon integration by parts:

$$\begin{aligned}\textstyle\int_{\mathrm{P}}\boldsymbol{v}\cdot\mathbf{curl}(\boldsymbol{x}_{\mathrm{P}}\wedge\boldsymbol{q}_k)\,\mathrm{dP} &= \textstyle\int_{\mathrm{P}}\mathbf{curl}\boldsymbol{v}\cdot(\boldsymbol{x}_{\mathrm{P}}\wedge\boldsymbol{q}_k)\,\mathrm{dP} + \int_{\partial\mathrm{P}}(\boldsymbol{v}\wedge\boldsymbol{n})\cdot(\boldsymbol{x}_{\mathrm{P}}\wedge\boldsymbol{q}_k)\,\mathrm{d}S\\ &= \textstyle\int_{\mathrm{P}}\mathbf{curl}\boldsymbol{v}\cdot(\boldsymbol{x}_{\mathrm{P}}\wedge\boldsymbol{q}_k)\,\mathrm{dP} + \int_{\partial\mathrm{P}}\Big(\boldsymbol{n}\wedge(\boldsymbol{x}_{\mathrm{P}}\wedge\boldsymbol{q}_k)\Big)\cdot\boldsymbol{v}\,\mathrm{d}S\\ &= \textstyle\int_{\mathrm{P}}\mathbf{curl}\boldsymbol{v}\cdot(\boldsymbol{x}_{\mathrm{P}}\wedge\boldsymbol{q}_k)\,\mathrm{dP} + \sum_f\int_f\Big(\boldsymbol{n}_f\wedge(\boldsymbol{x}_{\mathrm{P}}\wedge\boldsymbol{q}_k)\Big)^\tau\cdot\boldsymbol{v}^\tau\,\mathrm{d}f.\end{aligned} \tag{3.43}$$

The first term is given by the d.o.f. (3.41), and the second is computable as in (3.6). ∎

Hence, following the path of Remark 3.1 we can define a μ-dependent scalar product through the (Hilbert) norm

$$\|\boldsymbol{v}\|^2_{\mathrm{e},\mu,\mathrm{P}} := \|\mu^{1/2}\Pi^0_k \boldsymbol{v}\|^2_{0,\mathrm{P}} + h_{\mathrm{P}}\mu_0 \sum_i (dof_i\{(I-\Pi^0_k)\boldsymbol{v}\})^2, \tag{3.44}$$

or, for instance,

$$\|\boldsymbol{v}\|^2_{\mathrm{e},\mu,\mathrm{P}} := \|\mu^{1/2}\Pi^0_k \boldsymbol{v}\|^2_{0,\mathrm{P}} + h_{\mathrm{P}}\mu_0 \sum_{f\subset\partial\mathrm{P}} \|(I-\Pi^0_k)\boldsymbol{v}^\tau\|^2_{V^{\mathrm{e}}_k(f)} \tag{3.45}$$

getting, for positive constants α_*, α^* independent of h_{P},

$$\alpha_*\mu_0\|\boldsymbol{v}\|^2_{0,\mathrm{P}} \le \|\boldsymbol{v}\|^2_{e,\mu,\mathrm{P}} \le \alpha^*\mu_1\|\boldsymbol{v}\|_{0,\mathrm{P}} \qquad \forall \boldsymbol{v}\in V^{\mathrm{e}}_k(\mathrm{P}). \tag{3.46}$$

We observe that the associated scalar product will satisfy

$$[\boldsymbol{v},\boldsymbol{w}]_{0,\mathrm{P}} \le \Big([\boldsymbol{v},\boldsymbol{v}]_{\mathrm{e},\mu,\mathrm{P}}\Big)^{1/2}\Big([\boldsymbol{w},\boldsymbol{w}]_{\mathrm{e},\mu,\mathrm{P}}\Big)^{1/2} \le \mu_1\alpha^*\|\boldsymbol{v}\|_{0,\mathrm{P}}\|\boldsymbol{w}\|_{0,\mathrm{P}}, \tag{3.47}$$

$$[\boldsymbol{v},\mathbf{p}_k]_{\mathrm{e},\mu,\mathrm{P}} = \int_{\mathrm{P}} \mu\Pi^0_k\boldsymbol{v}\cdot\mathbf{p}_k\,\mathrm{dP} \qquad \forall\boldsymbol{v}\in V^{\mathrm{e}}_k(\mathrm{P}),\ \forall\mathbf{p}_k\in[\mathbb{P}_k(\mathrm{P})]^3. \tag{3.48}$$

In $V^{\mathrm{n}}_{k+1}(\mathrm{P})$ we have the degrees of freedom

- (3.49) • $\forall$ vertex ν the nodal value $q(\nu)$,
- (3.50) • $\forall$ edge e and $k\ge 1$ the moments $\int_e q\,p_{k-1}\,\mathrm{d}s \quad \forall p_{k-1}\in\mathbb{P}_{k-1}(e)$,
- (3.51) • $\forall$ face f with $\beta_f\ge 0$ the moments $\int_f(\nabla_f q\cdot\boldsymbol{x}_f)\,p_{\beta_f}\,\mathrm{d}f \quad \forall p_{\beta_f}\in\mathbb{P}_{\beta_f}(f)$,
- (3.52) • the moments $\int_{\mathrm{P}}\nabla q\cdot\boldsymbol{x}_{\mathrm{P}}\,p_{k-1}\,\mathrm{dP} \quad \forall p_{k-1}\in\mathbb{P}_{k-1}(\mathrm{P})$.

We point out (see [4]) that the degrees of freedom (3.49)-(3.51) on each face f allow to compute the $L^2(f)$-orthogonal projection operator from $SV^{\mathrm{n}}_{k+1}(f)$ to $\mathbb{P}_k(f)$. This, together with the degrees of freedom (3.52) and an integration by parts, gives us the $L^2(\mathrm{P})$-orthogonal projection operator from $V^{\mathrm{n}}_{k+1}(\mathrm{P})$ to $\mathbb{P}_{k-1}(\mathrm{P})$. Finally, for $V^{\mathrm{f}}_{k-1}(\mathrm{P})$ we have the degrees of freedom

- (3.53) • $\forall$ face f: $\int_f(\boldsymbol{w}\cdot\boldsymbol{n}_f)p_{k-1}\,\mathrm{d}f \quad \forall p_{k-1}\in\mathbb{P}_{k-1}(f)$,
- (3.54) • $\int_{\mathrm{P}}\boldsymbol{w}\cdot(\mathbf{grad}\,p_{k-1})\,\mathrm{dP} \quad \forall p_{k-1}\in\mathbb{P}_{k-1}(\mathrm{P})$, for $k>1$
- (3.55) • $\int_{\mathrm{P}}\boldsymbol{w}\cdot(\boldsymbol{x}_{\mathrm{P}}\wedge\mathbf{p}_k)\,\mathrm{dP} \quad \forall\mathbf{p}_k\in[\mathbb{P}_k(\mathrm{P})]^3$.

According to [12] we have now that from the above degrees of freedom we can compute the $[L^2(\mathrm{P})]^3$-orthogonal projection Π^0_s from $V^{\mathrm{f}}_{k-1}(\mathrm{P})$ to $[\mathbb{P}_s(\mathrm{P})]^3$ with $s\le k+1$.

In particular, along the same lines of Remark 3.1 we can define a scalar product $[\boldsymbol{w},\boldsymbol{v}]_{V^{\mathrm{f}}_{k-1}(\mathrm{P})}$ through the Hilbert norm

$$\|\boldsymbol{v}\|^2_{V^{\mathrm{f}}_{k-1}(\mathrm{P})} := \|\Pi^0_{k-1}\boldsymbol{v}\|^2_{0,\mathrm{P}} + h_{\mathrm{P}}\sum_f \|(I-\Pi^0_{k-1})\boldsymbol{v}\cdot\boldsymbol{n}_f\|^2_{0,f}, \tag{3.56}$$

and then there exist two positive constants α_1, α_2 independent of h_{P} such that

$$\alpha_1\|\boldsymbol{w}\|^2_{0,\mathrm{P}} \le \|\boldsymbol{w}\|^2_{V^{\mathrm{f}}_{k-1}(\mathrm{P})} \le \alpha_2\|\boldsymbol{w}\|^2_{0,\mathrm{P}} \qquad \forall\boldsymbol{w}\in V^{\mathrm{f}}_{k-1}(\mathrm{P}), \tag{3.57}$$

and also

$$[\boldsymbol{w}, \mathbf{p}_{k-1}]_{V^{\mathrm{f}}_{k-1}(\mathrm{P})} = (\boldsymbol{w}, \mathbf{p}_{k-1})_{0,\mathrm{P}} \qquad \forall \boldsymbol{w} \in V^{\mathrm{f}}_{k-1}(\mathrm{P}),\ \forall \mathbf{p}_{k-1} \in [\mathbb{P}_{k-1}(\mathrm{P})]^3. \tag{3.58}$$

Needless to say, instead of (3.56) we could also consider variants of the type of (3.7) and (3.44), using only the values dof_i of the degrees of freedom.

Note that $\mathbb{P}_{k+1}(\mathrm{P}) \subseteq V^{\mathrm{n}}_{k+1}(\mathrm{P})$, $[\mathbb{P}_k(\mathrm{P})]^3 \subseteq V^{\mathrm{e}}_k(\mathrm{P})$, and $[\mathbb{P}_{k-1}(\mathrm{P})]^3 \subseteq V^{\mathrm{f}}_{k-1}(\mathrm{P})$.

Proposition 3.8. It holds:

$$\mathbf{curl} V^{\mathrm{e}}_k(\mathrm{P}) = \{\boldsymbol{w} \in V^{\mathrm{f}}_{k-1}(\mathrm{P}) :\ \mathrm{div}\boldsymbol{w} = 0\}. \tag{3.59}$$

Proof. For every $\boldsymbol{v} \in V^{\mathrm{e}}_k(\mathrm{P})$ we have that $\boldsymbol{w} := \mathbf{curl}\, \boldsymbol{v}$ belongs to $V^{\mathrm{f}}_{k-1}(\mathrm{P})$. Indeed, on each face f we have that $\boldsymbol{w} \cdot \boldsymbol{n}_f \equiv \mathrm{rot}_f \boldsymbol{v}^\tau$ belongs to $\mathbb{P}_{k-1}(f)$ (see (3.2) and (3.29)), and moreover $\mathrm{div}\boldsymbol{w} = 0$ (obviously) and $\mathbf{curl}\boldsymbol{w} \in [\mathbb{P}_k(\mathrm{P})]^3$ from (3.27). Hence,

$$\mathbf{curl} V^{\mathrm{e}}_k(\mathrm{P}) \subseteq \{\boldsymbol{w} \in V^{\mathrm{f}}_{k-1}(\mathrm{P}) :\ \mathrm{div}\boldsymbol{w} = 0\}. \tag{3.60}$$

In order to prove the converse, we first note that from [9] we have that: if $\boldsymbol{w}$ is in $V^{\mathrm{f}}_{k-1}(\mathrm{P})$ with $\mathrm{div}\boldsymbol{w} = 0$, then $\boldsymbol{w} = \mathbf{curl}\boldsymbol{v}$ for some $\boldsymbol{v} \in \widetilde{V}^{\mathrm{e}}_k(\mathrm{P})$ (as defined in (3.32)). Then we use Proposition 3.5 and obtain a $\boldsymbol{v}^* \in V^{\mathrm{e}}_k(\mathrm{P})$ that, according to (3.34), has the same **curl**. An alternative proof could be derived by a simple dimensional count, following the same guidelines as in [6]. □

3.5. The global spaces. Let $\mathcal{T}_h$ be a decomposition of the computational domain Ω into polyhedra P. On $\mathcal{T}_h$ we make the following assumptions, quite standard in the VEM literature. We assume the existence of a positive constant γ such that any polyhedron P of the mesh (of diameter h_P) satisfies the following conditions:

$$\begin{aligned} &-\text{P is star-shaped with respect to a ball of radius bigger than } \gamma h_\mathrm{P};\\ &-\text{each face } f \text{ is star-shaped with respect to a ball of radius } \geq \gamma h_P,\\ &-\text{each edge has length bigger than } \gamma h_\mathrm{P}. \end{aligned} \tag{3.61}$$

We note that the first two conditions imply that P (and, respectively, every face of P) is simply connected. At the theoretical level, some of the above conditions could be avoided by using more technical arguments. We also point out that, at the practical level, as shown by the numerical tests of the Section 5, the third condition is negligible since the method seems very robust to degeneration of faces and edges. On the contrary, although the scheme is quite robust to distortion of the elements, the first condition is more relevant since extremely anisotropic element shapes can lead to poor results. Finally, as already mentioned, for simplicity we also assume that all the faces are convex.

We can now define the global nodal space:

$$V^{\mathrm{n}}_{k+1} \equiv V^{\mathrm{n}}_{k+1}(\Omega) := \Big\{ q \in H^1_0(\Omega) \text{ such that } q_{|\mathrm{P}} \in V^{\mathrm{n}}_{k+1}(\mathrm{P})\, \forall \mathrm{P} \in \mathcal{T}_h \Big\}, \tag{3.62}$$

with the obvious degrees of freedom

(3.63) • $\forall$ internal vertex ν the nodal value $q(\nu)$,

(3.64) • $\forall$ internal edge e and $k \geq 1$: $\int_e q\, p_{k-1}\, \mathrm{d}s \quad \forall p_{k-1} \in \mathbb{P}_{k-1}(e)$,

(3.65) • $\forall$ internal face f with $\beta_f \geq 0$: $\int_f (\nabla_f q \cdot \boldsymbol{x}_f) p_{\beta_f}\, \mathrm{d}f \quad \forall p_{\beta_f} \in \mathbb{P}_{\beta_f}(f)$,

(3.66) • $\forall$ element P, $k \geq 1$: $\int_\mathrm{P} \nabla q \cdot \boldsymbol{x}_\mathrm{P}\, p_{k-1}\, \mathrm{dP} \quad \forall p_{k-1} \in \mathbb{P}_{k-1}(\mathrm{P})$.

For the global edge space we have

$$V_k^{\mathrm{e}} \equiv V_k^{\mathrm{e}}(\Omega) := \left\{ \boldsymbol{v} \in H_0(\mathbf{curl};\Omega) \text{ such that } \boldsymbol{v}_{|\mathrm{P}} \in V_k^{\mathrm{e}}(\mathrm{P}) \, \forall \mathrm{P} \in \mathcal{T}_h \right\}, \tag{3.67}$$

with the obvious degrees of freedom

- (3.68) $\forall$ internal edge $e : \int_e (\boldsymbol{v} \cdot \boldsymbol{t}_e) p_k \, \mathrm{d}s \quad \forall p_k \in \mathbb{P}_k(e)$,
- (3.69) $\forall$ internal face f with $\beta_f \geq 0 : \int_f \boldsymbol{v}^\tau \cdot \boldsymbol{x}_f \, p_{\beta_f} \, \mathrm{d}f \quad \forall p_{\beta_f} \in \mathbb{P}_{\beta_f}(f)$,
- (3.70) $\forall$ internal face f: $\int_f \mathrm{rot}_f \boldsymbol{v}^\tau \, p_{k-1}^0 \, \mathrm{d}f \quad \forall p_{k-1}^0 \in \mathbb{P}_{k-1}^0(f) \qquad (\text{for } k > 1)$,
- (3.71) $\forall$ element P : $\int_{\mathrm{P}} (\boldsymbol{v} \cdot \boldsymbol{x}_{\mathrm{P}}) p_{k-1} \, \mathrm{dP} \quad \forall p_{k-1} \in \mathbb{P}_{k-1}(\mathrm{P})$,
- (3.72) $\forall$ element P : $\int_{\mathrm{P}} (\mathbf{curl}\boldsymbol{v}) \cdot (\boldsymbol{x}_{\mathrm{P}} \wedge \mathbf{p}_k) \, \mathrm{dP} \quad \forall \mathbf{p}_k \in [\mathbb{P}_k(\mathrm{P})]^3$.

Finally, for the global face space we have:

$$V_{k-1}^{\mathrm{f}} \equiv V_{k-1}^{\mathrm{f}}(\Omega) := \left\{ \boldsymbol{w} \in H_0(\mathrm{div};\Omega) \text{ such that } \boldsymbol{w}_{|\mathrm{P}} \in V_{k-1}^{\mathrm{f}}(\mathrm{P}) \, \forall \mathrm{P} \in \mathcal{T}_h \right\}, \tag{3.73}$$

with the degrees of freedom

- (3.74) $\forall$ internal face $f : \int_f (\boldsymbol{w} \cdot \boldsymbol{n}) p_{k-1} \, \mathrm{d}f \quad \forall p_{k-1} \in \mathbb{P}_{k-1}(f)$,
- (3.75) $\forall$ element P : $\int_{\mathrm{P}} \boldsymbol{w} \cdot (\boldsymbol{x}_{\mathrm{P}} \wedge \mathbf{p}_k) \, \mathrm{dP} \quad \forall \mathbf{p}_k \in [\mathbb{P}_k(\mathrm{P})]^3$,
- (3.76) $\forall$ element P : $\int_{\mathrm{P}} \boldsymbol{w} \cdot (\mathbf{grad} p_{k-1}) \, \mathrm{dP} \quad \forall p_{k-1} \in \mathbb{P}_{k-1}(\mathrm{P}) \quad k > 1$.

It is important to point out that

$$\nabla V_{k+1}^{\mathrm{n}} \subseteq V_k^{\mathrm{e}}. \tag{3.77}$$

In particular, it is easy to check that from Propositiom 3.6 it holds

$$\nabla V_{k+1}^{\mathrm{n}} \equiv \{ \boldsymbol{v} \in V_k^{\mathrm{e}} \text{ such that } \mathbf{curl}\boldsymbol{v} = 0 \}. \tag{3.78}$$

Similarly, also recalling Proposition 3.8, we easily have

$$\mathbf{curl} V_k^{\mathrm{e}} \subseteq V_{k-1}^{\mathrm{f}}. \tag{3.79}$$

For the converse we follow the same arguments of the proof of Proposition 3.8: first using [9], this time for the global spaces, and then correcting $\boldsymbol{v}$ with a $\nabla \xi$ which is single-valued on the faces. Hence

$$\mathbf{curl} V_k^{\mathrm{e}} \equiv \{ \boldsymbol{w} \in V_{k-1}^{\mathrm{f}} \text{ such that } \mathrm{div}\boldsymbol{w} = 0 \}. \tag{3.80}$$

Introducing the additional space (for *volume* 3-forms)

$$V_{k-1}^{\mathrm{v}} := \{ \gamma \in L^2(\Omega) \; \text{ such that } \gamma_{|\mathrm{P}} \in \mathbb{P}_{k-1}(\mathrm{P}) \, \forall \mathrm{P} \in \mathcal{T}_h \}, \tag{3.81}$$

we also have

$$\mathrm{div} V_{k-1}^{\mathrm{f}} \equiv V_{k-1}^{\mathrm{v}}. \tag{3.82}$$

Proposition 3.9. For the Virtual element spaces defined in (3.62), (3.67), (3.73), and (3.81) the following is an exact sequence:

$$\mathbb{R} \xrightarrow{\mathrm{i}} V_{k+1}^{\mathrm{n}}(\Omega) \xrightarrow{\mathbf{grad}} V_k^{\mathrm{e}}(\Omega) \xrightarrow{\mathbf{curl}} V_{k-1}^{\mathrm{f}}(\Omega) \xrightarrow{\mathrm{div}} V_{k-1}^{\mathrm{v}}(\Omega) \xrightarrow{\mathrm{o}} 0.$$

Remark 3.10. Here too it is very important to point out that the inclusions (3.77), (3.79) and (3.82) are (in a sense) also **practical**, and not only theoretical. By this, more specifically, we mean that: given the degrees of freedom of a $q \in V^{\rm n}_{k+1}$ we can compute the corresponding degrees of freedom of ∇q in $V^{\rm e}_k$; and given the degrees of freedom of a $\boldsymbol{v} \in V^{\rm e}_k$ we can compute the corresponding degrees of freedom of $\mathbf{curl}\,\boldsymbol{v}$ in $V^{\rm f}_{k-1}$; finally (and this is almost obvious) from the degrees of freedom of a $\boldsymbol{w} \in V^{\rm f}_{k-1}$ we can compute its divergence in each element and obtain an element in $V^{\rm v}_{k-1}$.

3.6. Scalar products for VEM spaces in 3D. From the local scalar products in $V^{\rm e}_k(\mathrm{P})$ we can also define a scalar product in $V^{\rm e}_k$ in the obvious way

$$[\boldsymbol{v},\boldsymbol{w}]_{e,\mu} := \sum_{\mathrm{P}\in\mathcal{T}_h} [\boldsymbol{v},\boldsymbol{w}]_{\mathrm{e},\mu,\mathrm{P}} \tag{3.83}$$

and we note that for some constants α_* and α^* independent of h

$$\alpha_*\mu_0(\boldsymbol{v},\boldsymbol{v})_{0,\Omega} \le [\boldsymbol{v},\boldsymbol{v}]_{e,\mu} \le \alpha^*\mu_1(\boldsymbol{v},\boldsymbol{v})_{0,\Omega} \qquad \forall \boldsymbol{v} \in V^{\rm e}_k. \tag{3.84}$$

It is also important to point out that, using (3.48) we have

$$[\boldsymbol{v},\boldsymbol{p}]_{e,\mu} = (\mu\Pi^0_k\boldsymbol{v},\boldsymbol{p})_{0,\Omega} \equiv \int_\Omega \mu\Pi^0_k\boldsymbol{v}\cdot\boldsymbol{p}\,\mathrm{d}\Omega \quad \forall\boldsymbol{v}\in V^{\rm e}_k,\ \forall\boldsymbol{p} \text{ piecewise in } (\mathbb{P}_k)^3. \tag{3.85}$$

From (3.56) we can also define a scalar product in $V^{\rm f}_{k-1}$ in the obvious way

$$[\boldsymbol{v},\boldsymbol{w}]_{V^{\rm f}_{k-1}} := \sum_{\mathrm{P}\in\mathcal{T}_h} [\boldsymbol{v},\boldsymbol{w}]_{V^{\rm f}_{k-1}(\mathrm{P})} \tag{3.86}$$

and we note that, for some constants α_1 and α_2 independent of h

$$\alpha_1(\boldsymbol{v},\boldsymbol{v})_{0,\Omega} \le [\boldsymbol{v},\boldsymbol{v}]_{V^{\rm f}_{k-1}} \le \alpha_2(\boldsymbol{v},\boldsymbol{v})_{0,\Omega} \qquad \forall\boldsymbol{v}\in V^{\rm f}_{k-1}. \tag{3.87}$$

Note also that, using (3.58) we have

$$[\boldsymbol{v},\boldsymbol{p}]_{V^{\rm f}_{k-1}} = (\boldsymbol{v},\boldsymbol{p})_{0,\Omega} \equiv \int_\Omega \boldsymbol{v}\cdot\boldsymbol{p}\,\mathrm{d}\Omega \qquad \forall\boldsymbol{v}\in V^{\rm f}_{k-1},\ \forall\boldsymbol{p} \text{ piecewise in } (\mathbb{P}_{k-1})^3. \tag{3.88}$$

4. The discrete problem and error estimates.

4.1. The discrete problem. Given $\boldsymbol{j} \in H_0(\mathrm{div};\Omega)$ with $\mathrm{div}\boldsymbol{j} = 0$, we construct its interpolant $\boldsymbol{j}_I \in V^{\rm f}_{k-1}$ that matches all the degrees of freedom (3.74)–(3.76):

$$\bullet\ \forall f : \textstyle\int_f((\boldsymbol{j}-\boldsymbol{j}_I)\cdot\boldsymbol{n})p_{k-1}\,\mathrm{d}f = 0\ \forall p_{k-1}\in\mathbb{P}_{k-1}(f), \tag{4.1}$$

$$\bullet\ \forall\mathrm{P} : \textstyle\int_\mathrm{P}(\boldsymbol{j}-\boldsymbol{j}_I)\cdot\mathbf{grad}\,p_{k-1}\,\mathrm{dP} = 0\ \forall p_{k-1}\in\mathbb{P}_{k-1}(\mathrm{P}), k>1 \tag{4.2}$$

$$\bullet\ \forall\mathrm{P} : \textstyle\int_\mathrm{P}(\boldsymbol{j}-\boldsymbol{j}_I)\cdot(\boldsymbol{x}_\mathrm{P}\wedge\mathbf{p}_k)\,\mathrm{dP} = 0\ \forall\mathbf{p}_k\in[\mathbb{P}_k(\mathrm{P})]^3. \tag{4.3}$$

Then we can introduce the **discretization** of (3.1):

$$\begin{cases} \text{find } \boldsymbol{H}_h \in V^{\rm e}_k \text{ and } p_h \in V^{\rm n}_{k+1} \text{ such that:} \\ [\mathbf{curl}\boldsymbol{H}_h,\mathbf{curl}\boldsymbol{v}]_{V^{\rm f}_{k-1}} + [\nabla p_h,\boldsymbol{v}]_{e,\mu} \ = \ [\boldsymbol{j}_I,\mathbf{curl}\boldsymbol{v}]_{V^{\rm f}_{k-1}} \quad \forall\boldsymbol{v}\in V^{\rm e}_k \\ [\nabla q,\boldsymbol{H}_h]_{e,\mu} \ = \ 0 \quad \forall q\in V^{\rm n}_{k+1}. \end{cases} \tag{4.4}$$

We point out that both $\mathbf{curl}\boldsymbol{H}_h$ and $\mathbf{curl}\boldsymbol{v}$ (as well as $\boldsymbol{j}_I$) are *face Virtual Elements in* $V^{\rm f}_{k-1}(\mathrm{P})$ in each polyhedron P, so that (taking also into account Remark 3.10) their *face* scalar products are computable as in (3.86). Similarly, from the degrees of freedom of a $q \in V^{\rm n}_{k+1}$ we can compute the degrees of freedom of ∇q, as an element of $V^{\rm e}_k$, so that the two edge-scalar products in (4.4) are computable as in (3.83).

Proposition 4.1. Problem (4.4) has a unique solution $(\boldsymbol{H}_h, p_h)$, and $p_h \equiv 0$.

Proof. Taking $\boldsymbol{v} = \nabla p_h$ (as we did for the continuous problem (3.1)) in the first equation, and using (3.84) we easily obtain $p_h \equiv 0$ for (4.4) as well. To prove uniqueness of $\boldsymbol{H}_h$, set $\boldsymbol{j}_I = 0$, and let $\overline{\boldsymbol{H}}_h$ be the solution of the homogeneous problem. From the first equation we deduce that $\mathbf{curl}\,\overline{\boldsymbol{H}}_h = 0$. Hence, from (3.78) we have $\overline{\boldsymbol{H}}_h = \nabla q_h^*$ for some $q_h^* \in V_{k+1}^n$. The second equation and (3.84) give then $\overline{\boldsymbol{H}}_h = 0$. ∎

In order to study the discretization error between (3.1) and (4.4) we need the interpolant $\boldsymbol{H}_I \in V_k^e$ of $\boldsymbol{H}$, defined through the degrees of freedom (3.68)-(3.72):

$$\bullet\ \forall\, e : \int_e ((\boldsymbol{H} - \boldsymbol{H}_I)\cdot \boldsymbol{t}_e) p_k \,\mathrm{d}s = 0 \quad \forall p_k \in \mathbb{P}_k(e), \tag{4.5}$$

$$\bullet\ \forall\, f : \int_f \mathrm{rot}_f (\boldsymbol{H} - \boldsymbol{H}_I)^\tau\, p_{k-1}^0 \,\mathrm{d}f = 0 \quad \forall p_{k-1}^0 \in \mathbb{P}_{k-1}^0(f) \text{ (for } k > 1), \tag{4.6}$$

$$\bullet\ \forall\, f \text{ with } \beta_f \geq 0 : \int_f ((\boldsymbol{H} - \boldsymbol{H}_I)^\tau \cdot \boldsymbol{x}_f) p_{\beta_f} \,\mathrm{d}f = 0 \quad \forall p_{\beta_f} \in \mathbb{P}_{\beta_f}(f), \tag{4.7}$$

$$\bullet\ \forall\, \mathrm{P} : \int_\mathrm{P} ((\boldsymbol{H} - \boldsymbol{H}_I)\cdot \boldsymbol{x}_\mathrm{P}) p_{k-1} \,\mathrm{dP} = 0 \quad \forall p_{k-1} \in \mathbb{P}_{k-1}(\mathrm{P}), \tag{4.8}$$

$$\bullet\ \forall\, \mathrm{P} : \int_\mathrm{P} \mathbf{curl}(\boldsymbol{H} - \boldsymbol{H}_I)\cdot (\boldsymbol{x}_\mathrm{P} \wedge \mathbf{p}_k) \,\mathrm{dP} = 0 \quad \forall \mathbf{p}_k \in [\mathbb{P}_k(\mathrm{P})]^3. \tag{4.9}$$

We have the following result.

Proposition 4.2. With the choices (4.1)-(4.3) and (4.5)-(4.9) we have

$$\mathbf{curl}(\boldsymbol{H}_I) = (\mathbf{curl}\boldsymbol{H})_I \equiv \boldsymbol{j}_I. \tag{4.10}$$

Proof. We should show that the *face degrees of freedom* (3.74)-(3.76) of the difference $\mathbf{curl}\boldsymbol{H}_I - \boldsymbol{j}_I$ are zero, that is:

$$\bullet\ \forall\, f : \int_f ((\mathbf{curl}\boldsymbol{H}_I - \boldsymbol{j}_I)\cdot \boldsymbol{n}) p_{k-1} \,\mathrm{d}f = 0 \quad \forall p_{k-1} \in \mathbb{P}_{k-1}(f), \tag{4.11}$$

$$\bullet\ \forall\, \mathrm{P} : \int_\mathrm{P} (\mathbf{curl}\boldsymbol{H}_I - \boldsymbol{j}_I)\cdot \mathbf{grad} p_{k-1} \,\mathrm{dP} = 0 \quad \forall p_{k-1} \in \mathbb{P}_{k-1}(\mathrm{P}), \tag{4.12}$$

$$\bullet\ \forall\, \mathrm{P} : \int_\mathrm{P} (\mathbf{curl}\boldsymbol{H}_I - \boldsymbol{j}_I)\cdot (\boldsymbol{x}_\mathrm{P} \wedge \mathbf{p}_k) \,\mathrm{dP} = 0 \quad \forall \mathbf{p}_k \in [\mathbb{P}_k(\mathrm{P})]^3. \tag{4.13}$$

From the interpolation formulas (4.1)-(4.3) we see that in (4.11)-(4.13) we can replace $\boldsymbol{j}_I$ with $\boldsymbol{j}$ (that in turn is equal to $\mathbf{curl}\boldsymbol{H}$). Hence (4.11)-(4.13) become

$$\bullet\ \forall f : \int_f \mathbf{curl}(\boldsymbol{H}_I - \boldsymbol{H})\cdot \boldsymbol{n}\, p_{k-1} \,\mathrm{d}f = 0\ \forall p_{k-1} \in \mathbb{P}_{k-1}(f), \tag{4.14}$$

$$\bullet\ \forall \mathrm{P} : \int_\mathrm{P} \mathbf{curl}(\boldsymbol{H}_I - \boldsymbol{H})\cdot \mathbf{grad} p_{k-1} \,\mathrm{dP} = 0\ \forall p_{k-1} \in \mathbb{P}_{k-1}(\mathrm{P}), \tag{4.15}$$

$$\bullet\ \forall \mathrm{P} : \int_\mathrm{P} \mathbf{curl}(\boldsymbol{H}_I - \boldsymbol{H})\cdot (\boldsymbol{x}_\mathrm{P} \wedge \mathbf{p}_k) \,\mathrm{dP} = 0\ \forall \mathbf{p}_k \in [\mathbb{P}_k(\mathrm{P})]^3. \tag{4.16}$$

Observing that (4.5) and (4.6) imply that

$$\int_f \mathrm{rot}_f (\boldsymbol{H} - \boldsymbol{H}_I)^\tau\, p_{k-1} \,\mathrm{d}f = 0 \quad \forall p_{k-1} \in \mathbb{P}_{k-1}(f),$$

and recalling that on each f the normal component of $\mathbf{curl}(\boldsymbol{H}_I - \boldsymbol{H})$ is equal to the rot_f of the tangential components $(\boldsymbol{H}_I - \boldsymbol{H})^\tau$, we deduce

$$\int_f \mathbf{curl}(\boldsymbol{H}_I - \boldsymbol{H})\cdot \boldsymbol{n} p_{k-1} \,\mathrm{d}f \equiv \int_f \mathrm{rot}_f (\boldsymbol{H}_I - \boldsymbol{H})^\tau\, p_{k-1} \,\mathrm{d}f = 0.$$

Hence, (4.14) is satisfied. Next, we note that, having already (4.14) on each face, the equation (4.15) follows immediately with an integration by parts on P. Finally, (4.16) is the same as (4.9), and the proof is concluded. ∎

We observe now that, once we know that $p_h = 0$, the first equation of (4.4) reads

$$[\mathbf{curl}\boldsymbol{H}_h, \mathbf{curl}\boldsymbol{v}]_{V^{\rm f}_{k-1}} = [\boldsymbol{j}_I, \mathbf{curl}\boldsymbol{v}]_{V^{\rm f}_{k-1}}\ \forall \boldsymbol{v}\in V^{\rm e}_k, \tag{4.17}$$

that in view of (4.10) becomes

$$[\mathbf{curl}\boldsymbol{H}_h - \mathbf{curl}\boldsymbol{H}_I, \mathbf{curl}\boldsymbol{v}]_{V^{\rm f}_{k-1}} = 0 \quad \forall \boldsymbol{v}\in V^{\rm e}_k. \tag{4.18}$$

Using $\boldsymbol{v} = \boldsymbol{H}_h - \boldsymbol{H}_I$ and (3.87), this easily implies

$$\mathbf{curl}\boldsymbol{H}_h = \mathbf{curl}\boldsymbol{H}_I = \boldsymbol{j}_I. \tag{4.19}$$

4.2. Commuting diagrams. Formula (4.10) represents, for $\boldsymbol{H}$ smooth, a commuting diagram property. Similar properties can be established also for the *nodal* and *face* interpolants. For a smooth function q, let q_I be its **nodal** interpolant in $V^{\rm n}_{k+1}(\mathrm{P})$ defined through the degrees of freedom (3.49)-(3.52), and let $(\nabla q)_I$ be the interpolant of ∇q in $V^{\rm e}_k(\mathrm{P})$ defined through the degrees of freedom (3.37)-(3.41). Since $\nabla q_I \in V^{\rm e}_k(\mathrm{P})$, to prove that $\nabla q_I \equiv (\nabla q)_I$ amounts to prove that the vector $\nabla q - \nabla q_I$ verifies

(4.20) • $\forall$ edge e: $\int_e \nabla(q-q_I)\cdot\boldsymbol{t}_e\, p_k\,{\rm d}s = 0 \quad \forall p_k\in\mathbb{P}_k(e)$,

(4.21) • $\forall$ face f with $\beta_f \geq 0$: $\int_f \nabla(q-q_I)^\tau\cdot\boldsymbol{x}_f\, p_{\beta_f}\,{\rm d}f = 0 \quad \forall p_{\beta_f}\in\mathbb{P}_{\beta_f}(f)$,

(4.22) • $\forall$ face f: $\int_f {\rm rot}_f\nabla(q-q_I)^\tau\, p^0_{k-1}\,{\rm d}f = 0 \quad \forall p^0_{k-1}\in\mathbb{P}^0_{k-1}(f)$ (for $k>1$),

(4.23) • $\int_{\mathrm{P}}(\nabla(q-q_I)\cdot\boldsymbol{x}_{\mathrm{P}})p_{k-1}\,{\rm dP} = 0 \quad \forall p_{k-1}\in\mathbb{P}_{k-1}(\mathrm{P})$,

(4.24) • $\int_{\mathrm{P}}(\mathbf{curl}\nabla(q-q_I))\cdot(\boldsymbol{x}_{\mathrm{P}}\wedge\mathbf{p}_k)\,{\rm dP} = 0 \quad \forall \mathbf{p}_k\in[\mathbb{P}_k(\mathrm{P})]^3$.

Conditions (4.21)–(4.24) are automatically verified. The only non-immediate condition is (4.20) which, integrating by parts and using (3.49)-(3.50), gives

$$\int_e \nabla(q-q_I)\cdot\boldsymbol{t}_e\, p_k\,{\rm d}s = -\int_e (q-q_I)\nabla p_k\cdot\boldsymbol{t}_e\,{\rm d}s = 0.$$

For the **face** interpolant it is even much easier. Looking at the degrees of freedom (3.74) and (3.76) we immediately see that: for every smooth enough vector field $\boldsymbol{w}$, denoting by $\boldsymbol{w}_I$ its interpolant in $V^{\rm f}_{k-1}(\mathrm{P})$ we have

$$\int_{\mathrm{P}} {\rm div}(\boldsymbol{w}-\boldsymbol{w}_I)p_{k-1}\,{\rm dP} = 0 \quad \forall p_{k-1}\in\mathbb{P}_{k-1}(\mathrm{P})$$

which immediately implies

$$\Pi^0_{k-1}{\rm div}\boldsymbol{w} = {\rm div}(\boldsymbol{w}_I) \tag{4.25}$$

that, in turn, can be interpreted as a commuting diagram if we consider Π^0_{k-1} as the interpolator from $L^2(\mathrm{P})$ to $\mathbb{P}_{k-1}(\mathrm{P})$.

4.3. Error estimates. Let us bound the error $\boldsymbol{H}-\boldsymbol{H}_h$ in terms of approximation errors for $\boldsymbol{H}$. From (4.19) we have

$$\mathbf{curl}(\boldsymbol{H}_I - \boldsymbol{H}_h) = 0, \tag{4.26}$$

and therefore, from (3.35),

$$\boldsymbol{H}_I - \boldsymbol{H}_h = \nabla q^*_h \text{ for some } q^*_h\in V^{\rm n}_{k+1}. \tag{4.27}$$

On the other hand, using (3.84) we have

$$\alpha_*\mu_0\|\boldsymbol{H}_I-\boldsymbol{H}_h\|^2_{0,\Omega}\le[\boldsymbol{H}_I-\boldsymbol{H}_h,\boldsymbol{H}_I-\boldsymbol{H}_h]_{e,\mu}. \tag{4.28}$$

Then:

$$\begin{aligned}
&\alpha_*\mu_0\|\boldsymbol{H}_I-\boldsymbol{H}_h\|^2_{0,\Omega}\le[\boldsymbol{H}_I-\boldsymbol{H}_h,\boldsymbol{H}_I-\boldsymbol{H}_h]_{e,\mu}\\
&\;=\!(\text{use (4.27)})\;[\boldsymbol{H}_I-\boldsymbol{H}_h,\nabla q_h^*]_{e,\mu}\\
&\;=\!(\text{use the second of (4.4)})\;[\boldsymbol{H}_I,\nabla q_h^*]_{e,\mu}\\
&\;=\!(\text{add and subtract }\Pi^0_k\boldsymbol{H})\;[\boldsymbol{H}_I-\Pi^0_k\boldsymbol{H},\nabla q_h^*]_{e,\mu}+[\Pi^0_k\boldsymbol{H},\nabla q_h^*]_{e,\mu}\\
&\;=\!(\text{use (3.85)})\;[\boldsymbol{H}_I-\Pi^0_k\boldsymbol{H},\nabla q_h^*]_{e,\mu}+(\Pi^0_k\boldsymbol{H},\mu\Pi^0_k\nabla q_h^*)_{0,\Omega}\\
&\;=\!(\text{use the 2}^{\text{nd}}\text{ of (3.1)})\;\underbrace{[\boldsymbol{H}_I-\Pi^0_k\boldsymbol{H},\nabla q_h^*]_{e,\mu}}_{I}+\underbrace{(\Pi^0_k\boldsymbol{H},\mu\Pi^0_k\nabla q_h^*)_{0,\Omega}-(\boldsymbol{H},\mu\nabla q_h^*)_{0,\Omega}}_{II}
\end{aligned}$$

For the first term we use (3.47) to get

$$I\le\mu_1\alpha^*\|\boldsymbol{H}_I-\Pi^0_k\boldsymbol{H}\|_{0,\Omega}\|\nabla q_h^*\|_{0,\Omega}. \tag{4.29}$$

Next, following arguments similar to [11] (Lemma 5.3), we obtain:

$$\begin{aligned}
II&=(\Pi^0_k\boldsymbol{H},\mu\Pi^0_k\nabla q_h^*)_{0,\Omega}-(\boldsymbol{H},\mu\nabla q_h^*)_{0,\Omega}+(\boldsymbol{H},\mu\Pi^0_k\nabla q_h^*)_{0,\Omega}-(\boldsymbol{H},\mu\Pi^0_k\nabla q_h^*)_{0,\Omega}\\
&=(\Pi^0_k\boldsymbol{H}-\boldsymbol{H},\mu\Pi^0_k\nabla q_h^*)_{0,\Omega}+(\mu\boldsymbol{H},\Pi^0_k\nabla q_h^*-\nabla q_h^*)_{0,\Omega}\\
&=(\Pi^0_k\boldsymbol{H}-\boldsymbol{H},\mu\Pi^0_k\nabla q_h^*)_{0,\Omega}+(\mu\boldsymbol{H}-\Pi^0_k\mu\boldsymbol{H},\Pi^0_k\nabla q_h^*-\nabla q_h^*)_{0,\Omega} \qquad (4.30)\\
&\le\|\Pi^0_k\boldsymbol{H}-\boldsymbol{H}\|_{0,\Omega}\|\mu\Pi^0_k\nabla q_h^*\|_{0,\Omega}+\|\mu\boldsymbol{H}-\Pi^0_k\mu\boldsymbol{H}\|_{0,\Omega}\|\Pi^0_k\nabla q_h^*-\nabla q_h^*\|_{0,\Omega}\\
&\le\mu_1\|\Pi^0_k\boldsymbol{H}-\boldsymbol{H}\|_{0,\Omega}\|\nabla q_h^*\|_{0,\Omega}+\|\mu\boldsymbol{H}-\Pi^0_k\mu\boldsymbol{H}\|_{0,\Omega}\|\nabla q_h^*\|_{0,\Omega}.
\end{aligned}$$

Inserting (4.29)-(4.30) in the above estimate we deduce

$$\begin{aligned}
&\alpha_*\mu_0\|\boldsymbol{H}_I-\boldsymbol{H}_h\|^2_{0,\Omega}\le\\
&\qquad\Big(\mu_1\alpha^*\|\boldsymbol{H}_I-\Pi^0_k\boldsymbol{H}\|_{0,\Omega}+\mu_1\|\Pi^0_k\boldsymbol{H}-\boldsymbol{H}\|_{0,\Omega}+\|\mu\boldsymbol{H}-\Pi^0_k\mu\boldsymbol{H}\|_{0,\Omega}\Big)\|\nabla q_h^*\|_{0,\Omega}
\end{aligned}$$

that implies immediately (since $\alpha^*\ge1$)

$$\|\boldsymbol{H}_I-\boldsymbol{H}_h\|_{0,\Omega}\le\frac{\mu_1\alpha^*}{\mu_0\alpha_*}\Big(\|\boldsymbol{H}_I-\Pi^0_k\boldsymbol{H}\|_{0,\Omega}+\|\Pi^0_k\boldsymbol{H}-\boldsymbol{H}\|_{0,\Omega}\Big)+\frac{1}{\mu_0\alpha_*}\|\mu\boldsymbol{H}-\Pi^0_k\mu\boldsymbol{H}\|_{0,\Omega}.$$

Summarizing:

Theorem 4.3. Problem (4.4) has a unique solution, and we have

$$\|\boldsymbol{H}-\boldsymbol{H}_h\|_{0,\Omega}\le C\Big(\|\boldsymbol{H}-\boldsymbol{H}_I\|_{0,\Omega}+\|\Pi^0_k\boldsymbol{H}-\boldsymbol{H}\|_{0,\Omega}+\|\mu\boldsymbol{H}-\Pi^0_k(\mu\boldsymbol{H})\|_{0,\Omega}\Big), \tag{4.31}$$

with C a constant depending on μ but independent of the mesh size. Moreover,

$$\|\mathbf{curl}(\boldsymbol{H}-\boldsymbol{H}_h)\|_{0,\Omega}=\|\boldsymbol{j}-\boldsymbol{j}_I\|_{0,\Omega}. \tag{4.32}$$

Remark 4.4. The error bounds in (4.31) and (4.32) imply that the approximation error is of the same order (up to a multiplicative constant independent of h) of the interpolation error. The last two terms of (4.31) can be bounded using classical polynomial approximation properties. In particular, if the data μ and the solution $\mathbf{H}$ are sufficiently regular, one has that the **projection** errors (namely, the last two terms in (4.31)) can be estimated by

$$\|\boldsymbol{H} - \Pi_k^0 \boldsymbol{H}\|_{0,\Omega} + \|\mu \boldsymbol{H} - \Pi_k^0(\mu \boldsymbol{H})\|_{0,\Omega} \le C h^s \|\boldsymbol{H}\|_{s,\Omega} \qquad 0 \le s \le k+1, \tag{4.33}$$

where the constant C depends only on the polynomial degree k, the mesh regularity parameter γ, and $\|\mu\|_{W^{k+1,\infty}(\Omega_h)}$. On the other hand, **interpolation** estimates for 3d vector valued VEMs are still *in fieri*, as far as we know, in the international VEM community. However, a widely shared *educated guess* is that an estimate like (4.33) would also hold for $\|\boldsymbol{H} - \boldsymbol{H}_I\|_{0,\Omega}$, taking also into account that our local spaces contain all polynomials of degree k. The proof should be obtainable by tools similar to those already developed and used so far for VEMs (see, e.g., [16, 14, 38, 19, 18, 23]). The main difficulty, apparently, lies in the great variety of vector valued VEM spaces (splitting the proofs in zillions of different rivulets, each dealing with a very particular case) as well as in the great variety of possible geometric properties of the polyhedral elements used in the decomposition. Such a proof goes way beyond the scopes of the present paper, and we decided to stick on (4.31) that can still be seen as an "optimality result".

The same is true for the error (4.32), which is already an interpolation error. Note however that here we are dealing with spaces similar to Nedéléc second types elements, where the order of approximation of the $\boldsymbol{H}$ field is one level higher than that of its **curl**, so that in a possible estimate of the error in the $H(\mathbf{curl};\Omega)$-norm the error would be dominated by the **curl** part, that however is the less crucial of the two, since it deals with the approximation of a *known datum* and not of the (unknown) solution of the system of equations. □

Remark 4.5. By inspecting the proof of Theorem 4.3 we notice that, for this particular problem, the consistency property (3.88) for the space V^{f}_{k-1} is never used. Since only property (3.87) is needed, in V^{f}_{k-1} we could simply take, for instance, as *scalar product in* V^{f}_{k-1} the one (much cheaper to compute) associated to the norm

$$\|\boldsymbol{v}\|^2_{V^{\mathrm{f}}_{k-1}} := \sum_i (dof_i(\boldsymbol{v}))^2, \tag{4.34}$$

where dof_i are the degrees of freedom in V^{f}_{k-1} properly scaled.

5. Numerical Results.

In this section we numerically validate the proposed VEM approach. More precisely, we will focus on two main aspects of this method. We will first show that we recover the theoretical convergence rate for standard and serendipity VEM, then we compare these two approaches in terms of number of degrees of freedom. For the present study we consider the cases $k = 1$ and $k = 2$. A lowest order case (not belonging to the present family) has been already discussed in [6].

In the following two tests we use four different types of decompositions of $[0, 1]^3$:

- **Cube**, a mesh composed by cubes;
- **Nine**, a regular mesh composed by 9-faced polyhedrons in accordance with a periodic pattern;
- **CVT**, a Voronoi tessellation obtained by a standard Lloyd algorithm [32];

- **Random**, a Voronoi tessellation associated with a set of seeds randomly distributed inside Ω.

Note that the meshes taken into account are of increasing complexity; in particular, the meshes **CVT** and **Random** have polyhedra with small faces and edges.

All discretizations have been generated with the c++ library `voro++` [42] and we exploit the software PARDISO [41, 40] to solve the resulting linear systems. In order to

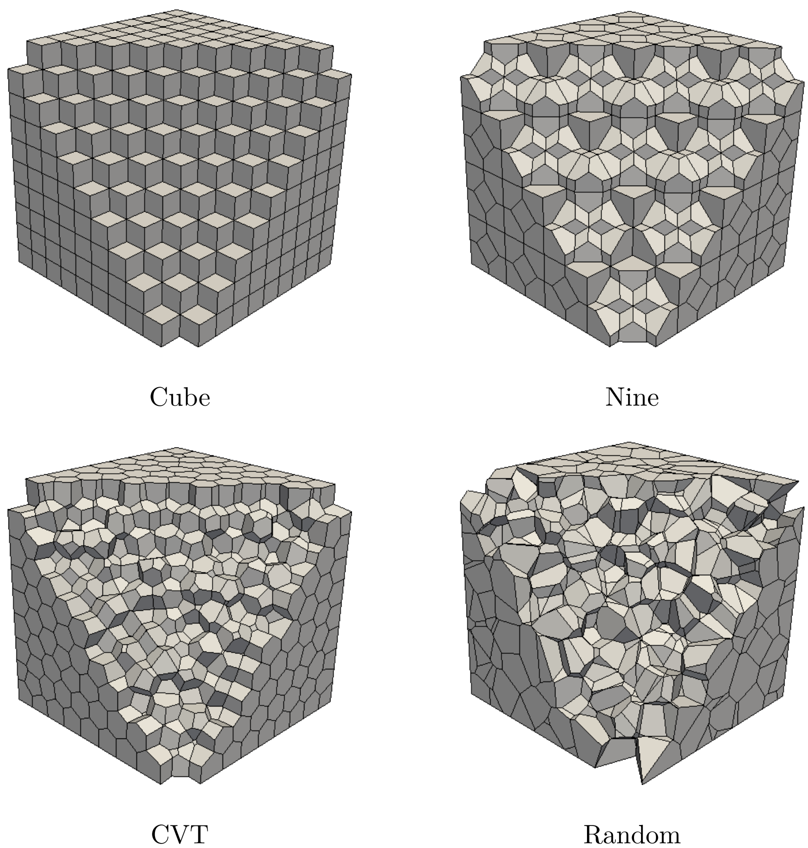

FIGURE 1. *A sample of the used meshes.*

study the error convergence rate, for each type of mesh we consider a sequence of three progressive refinements composed by approximately 27, 125 and 1000 polyhedrons. Then, we associate with each mesh a mesh-size

$$h := \frac{1}{N_{\mathrm{P}}} \sum_{i=1}^{N_{\mathrm{P}}} h_{\mathrm{P}}\,,$$

where N_{P} is the number of polyhedrons P in the mesh and h_{P} is the diameter of P.

Since $\boldsymbol{H}_h$ is virtual, we use its projection $\Pi^0_k \boldsymbol{H}_h$ to compute the L^2-error, i.e., the following quantity is used as an indicator of the L^2-error:

$$\frac{||\boldsymbol{H} - \Pi^0_k \boldsymbol{H}_h||_{0,\Omega}}{||\boldsymbol{H}||_{0,\Omega}}\,.$$

The expected convergence rate is $O(h^{k+1})$.

Test case 1: h-analysis

We consider a problem with a constant permeability $\mu(\mathbf{x}) = 1$. We take as exact solution

$$\boldsymbol{H}(x,\, y,\, z) := \frac{1}{\pi} \begin{pmatrix} \sin(\pi y) - \sin(\pi z) \\ \sin(\pi z) - \sin(\pi x) \\ \sin(\pi x) - \sin(\pi y) \end{pmatrix},$$

and chose right-hand side and boundary conditions accordingly.

In Figure 2 we show the convergence curves for each set of meshes. The error behaves as expected ($O(h^2)$ and $O(h^3)$ for $k = 1$ and $k = 2$, respectively).

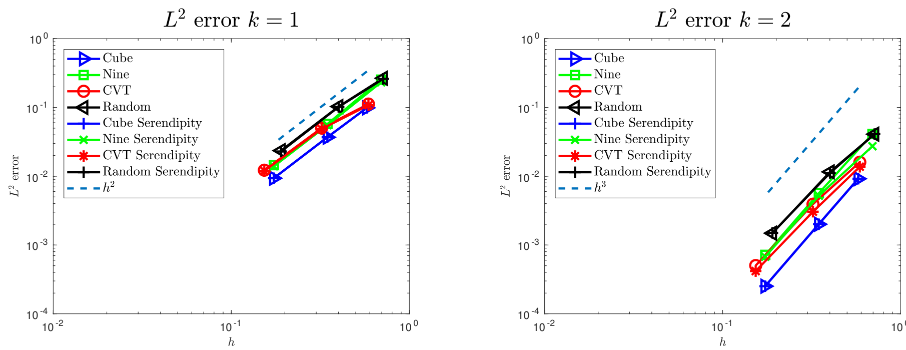

FIGURE 2. *Test case 1: L^2-error for standard and serendipity approach: case $k = 1$ and $k = 2$.*

From Figure 2 we also observe that we get almost the same values when we consider the standard or the serendipity approach. These two methods are equivalent in terms of error, but the serendipity approach requires fewer degrees of freedom. To better quantify the gain in terms of computational effort, we compute the quantity

$$\texttt{gain} := \frac{\#dof_f - \#dof_f^S}{\#dof_f}\, 100\%\,,$$

where $\#dof_f$ and $\#dof_f^S$ are the number of degrees of freedom on the faces in standard and serendipity VEM, respectively. We underline that in this computation we do not take into account the internal degrees of freedom since they can be removed via static condensation. As we can see from the data in Table 1, the gain is remarkable (almost 50% of the face d.o.f.s). Note that this also reflects on a much better performance of several solvers of the final linear system.

gain

	$k=1$				$k=2$			
$\sim N_P$	Cube	Nine	CVT	Random	Cube	Nine	CVT	Random
27	56.6%	51.0%	50.2%	50.3%	56.4%	52.0%	49.9%	50.4%
125	59.5%	53.6%	50.5%	50.1%	58.5%	54.1%	51.6%	50.2%
1000	61.8%	54.9%	50.3%	49.8%	60.2%	55.0%	44.3%	49.9%

TABLE 1
Test case 1: values of gain *for each type of mesh taken into account.*

If we compare the total number of degrees of freedom, i.e., including the internal ones, the gain in percentage is obviously smaller, since we are applying serendipity only on faces. For instance, in the case of the 125 CVT mesh and $k = 2$ one gets 40.7% instead of 51.6% (and similarly in the other cases). We nevertheless remind that, for the reasons explained above, counting only the degrees of freedom on faces is a better estimation of the overall computational cost.

Test case 2: h-analysis with a variable $\mu(\mathbf{x})$

We consider now a problem with variable permeability $\mu(\mathbf{x})$ given by

$$\mu(x, y, z) := 1 + x + y + z.$$

We take as exact solution

$$\boldsymbol{H}(x, y, z) := \frac{1}{(1 + x + y + z)} \begin{pmatrix} \sin(\pi y) \\ \sin(\pi z) \\ \sin(\pi x) \end{pmatrix},$$

and we choose again right-hand side and boundary conditions accordingly. In Figure 3 we provide the convergence curves for each set of meshes. The L^2-error behaves again as expected.

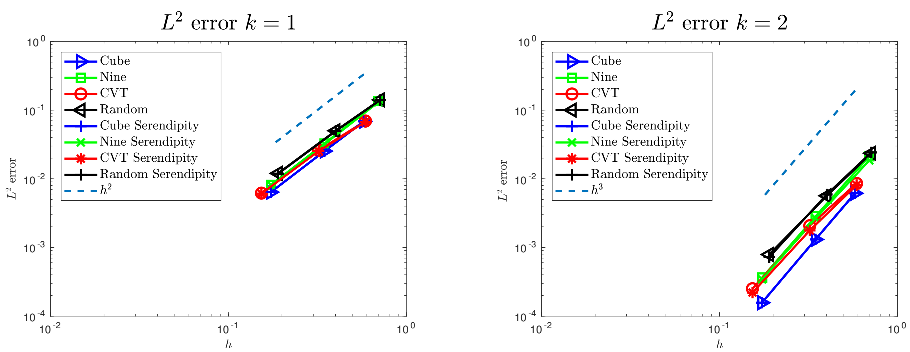

FIGURE 3. *Test case 2 - L^2-error for standard and serendipity approach: case $k = 1$ and $k = 2$.*

REFERENCES

[1] B. Ahmad, A. Alsaedi, F. Brezzi, L. D. Marini, and A. Russo, *Equivalent projectors for virtual element methods*, Comput. Math. Appl., 66 (2013), pp. 376–391.

[2] D. N. Arnold, F. Brezzi, B. Cockburn, and L. D. Marini, *Unified analysis of discontinuous Galerkin methods for elliptic problems*, SIAM J. Numer. Anal., 39 (2001), pp. 1749–1779.

[3] E. Artioli, S. de Miranda, C. Lovadina, and L. Patruno, *A stress/displacement virtual element method for plane elasticity problems*, Comput. Methods Appl. Mech. Engrg., 325 (2017), pp. 155–174.

[4] L. Beirão da Veiga, F. Brezzi, F. Dassi, L. D. Marini, and A. Russo, *Virtual Element approximation of 2D magnetostatic problems*, Comput. Methods Appl. Mech. Engrg., 327 (2017), pp. 173–195.

[5] L. Beirão da Veiga, F. Brezzi, A. Cangiani, G. Manzini, L. D. Marini, and A. Russo, *Basic principles of virtual element methods*, Math. Models Methods Appl. Sci., 23 (2013), pp. 199–214.

[6] L. Beirão da Veiga, F. Brezzi, F. Dassi, L. D. Marini, and A. Russo, *Lowest order virtual element approximation of magnetostatic problems*, Comput. Methods Appl. Mech. Engrg., 332 (2018), pp. 343–362.

[7] L. Beirão da Veiga, F. Brezzi, and L. D. Marini, *Virtual elements for linear elasticity problems*, SIAM J. Numer. Anal., 51 (2013), pp. 794–812.

[8] L. Beirão da Veiga, F. Brezzi, L. D. Marini, and A. Russo, *The hitchhiker's guide to the virtual element method*, Math. Models Methods Appl. Sci., 24 (2014), pp. 1541–1573.
[9] L. Beirão da Veiga, F. Brezzi, L. D. Marini, and A. Russo, *$H(div)$ and $H(curl)$-conforming VEM*, Numer. Math., 133 (2016), pp. 303–332.
[10] L. Beirão da Veiga, F. Brezzi, L. D. Marini, and A. Russo, *Serendipity nodal VEM spaces*, Comp. Fluids, 141 (2016), pp. 2–12.
[11] L. Beirão da Veiga, F. Brezzi, L. D. Marini, and A. Russo, *Virtual element methods for general second order elliptic problems on polygonal meshes*, Math. Models Methods Appl. Sci., 26 (2016), pp. 729–750.
[12] L. Beirão da Veiga, F. Brezzi, L. D. Marini, and A. Russo, *Serendipity face and edge VEM spaces*, Rend. Lincei Mat. Appl., 28 (2017), pp. 143–180.
[13] L. Beirão da Veiga, K. Lipnikov, and G. Manzini, *The mimetic finite difference method for elliptic problems*, vol. 11 of MS&A. Modeling, Simulation and Applications, Springer, Cham, 2014.
[14] L. Beirão da Veiga, C. Lovadina, and A. Russo, *Stability analysis for the virtual element method*, Math. Models Methods Appl. Sci., 27 (2017), pp. 2557 – 2594.
[15] L. Beirão da Veiga, C. Lovadina, and G. Vacca, *Divergence free Virtual Elements for the Stokes problem on polygonal meshes*, ESAIM Math. Model. Numer. Anal., 51 (2017), pp. 509–535.
[16] L. Beirão da Veiga, D. Mora, G. Rivera, and R. Rodríguez, *A virtual element method for the acoustic vibration problem*, Numer. Math., 136 (2017), pp. 725–736.
[17] M. F. Benedetto, S. Berrone, S. Pieraccini, and S. Scialò, *The virtual element method for discrete fracture network simulations*, Comput. Methods Appl. Mech. Engrg., 280 (2014), pp. 135–156.
[18] S. Brenner and L. Sung, *Virtual Element Methods on meshes with small edges or faces*, Math. Models Methods Appl. Sci., 28 (2018), pp. 1291–1336.
[19] S. C. Brenner, Q. Guan, and L.-Y. Sung, *Some estimates for virtual element methods*, Comput. Methods Appl. Math., 17 (2017), pp. 553–574.
[20] F. Brezzi, R. S. Falk, and L. D. Marini, *Basic principles of mixed virtual element methods*, ESAIM Math. Model. Numer. Anal., 48 (2014), pp. 1227–1240.
[21] F. Brezzi and L. D. Marini, *Virtual element methods for plate bending problems*, Comput. Methods Appl. Mech. Engrg., 253 (2013), pp. 455–462.
[22] E. Cáceres and G. N. Gatica, *A mixed virtual element method for the pseudostress-velocity formulation of the Stokes problem*, IMA J. Numer. Anal., 37 (2017), pp. 296–331.
[23] L. Chen and J. Huang, *Some error analysis on virtual element methods*, CALCOLO 55(5) (2018) https://doi.org/10.1007/s1009
[24] B. Cockburn, *Discontinuous Galerkin methods*, ZAMM Z. Angew. Math. Mech, 83 (2003), pp. 731–754.
[25] B. Cockburn, D.A. Di Pietro, and A. Ern, *Bridging the hybrid high-order and hybridizable discontinuous Galerkin methods*, ESAIM Math. Model. Numer. Anal., 50 (2016), pp. 635–650.
[26] B. Cockburn, J. Gopalakrishnan, and R. Lazarov, *Unified hybridization of discontinuous Galerkin, mixed, and continuous Galerkin methods for second order elliptic problems*, SIAM J. Numer. Anal., 47 (2009), pp. 1319–1365.
[27] L. Demkowicz, P. Monk, L. Vardapetyan, and W. Rachowicz, *De Rham diagram for hp finite element spaces*, Comput. Methods Appl. Mech. Engrg., 39 (2000), pp. 29–38.
[28] D.A. Di Pietro, B. Kapidani, R. Specogna, and F. Trevisan, *An arbitrary-order discontinuous skeletal method for solving electrostatics on general polyhedral meshes*, IEEE Transactions on Magnetics, 53 (2017), pp. 1–4.
[29] V. Dolejší and M. Feistauer, *Discontinuous Galerkin method. Analysis and applications to compressible flow*, vol. 48 of Springer Series in Computational Mathematics, Springer, Cham, 2015.
[30] J. Droniou, R. Eymard, T. Gallouët, and R. Herbin, *A unified approach to mimetic finite difference, hybrid finite volume and mixed finite volume methods*, Math. Models Methods Appl. Sci., 20 (2010), pp. 265–295.
[31] J. Droniou, R. Eymard, T. Gallouët, and R. Herbin, *Gradient schemes: a generic framework for the discretisation of linear, nonlinear and nonlocal elliptic and parabolic equations*, Math. Models Methods Appl. Sci., 23 (2013), pp. 2395–2432.
[32] Q. Du, V. Faber, and M. Gunzburger, *Centroidal Voronoi tessellations: Applications and algorithms*, SIAM Rev., 41 (1999), pp. 637–676.
[33] M. S. Floater, *Generalized barycentric coordinates and applications*, Acta Numer., 24 (2015), pp. 215–258.

[34] A. L. Gain, C. Talischi, and G. H. Paulino, *On the Virtual Element Method for three-dimensional linear elasticity problems on arbitrary polyhedral meshes*, Comput. Methods Appl. Mech. Engrg., 282 (2014), pp. 132–160.

[35] H. Kanayama, R. Motoyama, K. Endo, and F. Kikuchi, *Three dimensional magnetostatic analysis using Nédélec's elements*, IEEE Transactions on Magnetics, 26 (1990), pp. 682–685.

[36] F. Kikuchi, *Mixed formulations for finite element analysis of magnetostatic and electrostatic problems*, Japan J. Appl. Math., 6 (1989), pp. 209–221.

[37] K. Lipnikov, G. Manzini, and M. Shashkov, *Mimetic finite difference method*, J. Comput. Phys., 257 (2014), pp. 1163–1227.

[38] D. Mora, G. Rivera, and R. Rodríguez, *A virtual element method for the Steklov eigenvalue problem*, Math. Models Methods Appl. Sci., 25 (2015), pp. 1421–1445.

[39] I. Perugia, P. Pietra, and A. Russo, *A plane wave virtual element method for the Helmholtz problem*, ESAIM Math. Model. Numer. Anal., 50 (2016), pp. 783–808.

[40] C. Petra, O. Schenk, and M. Anitescu, *Real-time stochastic optimization of complex energy systems on high-performance computers*, IEEE Computing in Science & Engineering, 16 (2014), pp. 32–42.

[41] C. Petra, O. Schenk, M. Lubin, and K. Gärtner, *An augmented incomplete factorization approach for computing the Schur complement in stochastic optimization*, SIAM Journal on Scientific Computing, 36 (2014), pp. C139–C162.

[42] C. Rycroft, *Voro++: A three-dimensional Voronoi cell library in c++*, Chaos, 19 (2009), p. 041111.

[43] N. Sukumar and E. A. Malsch, *Recent advances in the construction of polygonal finite element interpolants*, Arch. Comput. Methods Engrg., 13 (2006), pp. 129–163.

[44] C. Talischi, G. H. Paulino, A. Pereira, and I. F. M. Menezes, *Polygonal finite elements for topology optimization: A unifying paradigm*, Internat. J. Numer. Methods Engrg., 82 (2010), pp. 671–698.

[45] E. Wachspress, *Rational bases for convex polyhedra*, Comput. Math. Appl., 59 (2010), pp. 1953–1956.

[46] P. Wriggers, W. T. Rust, B. D. Reddy, , *A virtual element method for contact*, Computational Mechanics, 58 (2016), pp. 1039–1050.

[47] P. Wriggers, W. T. Rust, B. D. Reddy, and B. Hudobivnik, *Efficient virtual element formulations for compressible and incompressible finite deformations*, Computational Mechanics, 60 (2017), pp. 253–268.